

---

# Diversity as a Reward: Fine-Tuning LLMs on a Mixture of Domain-Undetermined Data

---

Zhenqing Ling<sup>\*1</sup> Daoyuan Chen<sup>\*2</sup> Liuyi Yao<sup>2</sup> Yaliang Li<sup>2</sup> Ying Shen<sup>1</sup>

## Abstract

Fine-tuning large language models (LLMs) using diverse datasets is crucial for enhancing their overall performance across various domains. In practical scenarios, existing methods based on modeling the mixture proportions of data composition often struggle with data whose domain labels are missing, imprecise or non-normalized, while methods based on data selection usually encounter difficulties in balancing multi-domain performance. To address these challenges, in this paper, we study the role of data diversity in enhancing the overall abilities of LLMs by empirically constructing contrastive data pools and theoretically deriving explanations for both inter- and intra-diversity. Building upon the insights gained, we propose a new method that gives the LLM a dual identity: an output model to cognitively probe and select data based on diversity reward, as well as an input model to be tuned with the selected data. Extensive experiments show that the proposed method notably boosts performance across domain-undetermined data and a series of foundational downstream tasks when applied to various advanced LLMs. We release our code and hope this study can shed light on the understanding of data diversity and advance feedback-driven data-model co-development for LLMs.

## 1. Introduction

The advancement of large language models (LLMs), exemplified by open-source models such as the Llama3 series (Dubey et al., 2024), Qwen2 series (Yang et al., 2024), and the DeepSeek-V3 series (Liu et al., 2024a), along with closed-source models such as GPT-4 (Achiam et al., 2023), has revolutionized artificial intelligence by enhancing capabilities in foundational abilities such as common sense, rea-

soning, mathematics, and coding. Fine-tuning these models further optimizes their usability by enhancing their performance and aligning with specific human instructions and preferences (Taori et al., 2023; Rafailov et al., 2023).

To cultivate comprehensive capabilities in LLMs, fruitful studies have explored preferable trade-offs between quality, quantity, and diversity of their training data (Li et al., 2024b; Chen et al., 2024b; Qin et al., 2024; Zhao et al., 2024a). For example, methods focusing on data selection (Li et al., 2024a; Xia et al., 2024; Wang et al., 2023) and mixture (Ge et al., 2024) demonstrate promising capabilities to enhance model performance, particularly through semantic diversity (Lu et al., 2024; Liu et al., 2024b).

However, real-world applications frequently encounter unlabeled data and difficulties in domain labeling (Ge et al., 2023), posing challenges for data mixture methodologies that take the domain tags as a prior, as well as the data selection approaches, which often prioritize quality over diversity especially with data sourced from quite different domains.

To leverage the best of both worlds, in this work, we propose a new fine-tuning method for LLMs named **DAAR**, which encourages the given model to learn **diversity as a reward** signal, and then to autonomously select domain-undetermined training data to achieve a theoretically informed trade-off to maximize diversity for overall model performance enhancement.

Our investigation begins by diving into the semantic diversity of LLM data, considering how to explicitly model it and how it can influence the overall performance of LLMs. We systematically construct contrastive data pools and conduct extensive empirical examinations of different distributional performances across various foundational LLM capabilities. Based on these observations, we provide theoretical discussions on a general assumption that a mixture of underlying component LLMs determines the data mixing effect, and the explanations regarding inter- and intra-diversity modeled from a data semantic perspective.

Our theoretical insights illuminate that optimal solutions for overall model performance enhancement cannot be explicitly applied to domain-undetermined data. To address this, we integrate an external multi-layer perceptron (MLP) struc-

<sup>\*</sup>Equal contribution <sup>1</sup>Sun Yat-sen University, China  
<sup>2</sup>Alibaba Group, China. Correspondence to: Ying Shen <sheny76@mail.sysu.edu.cn>.

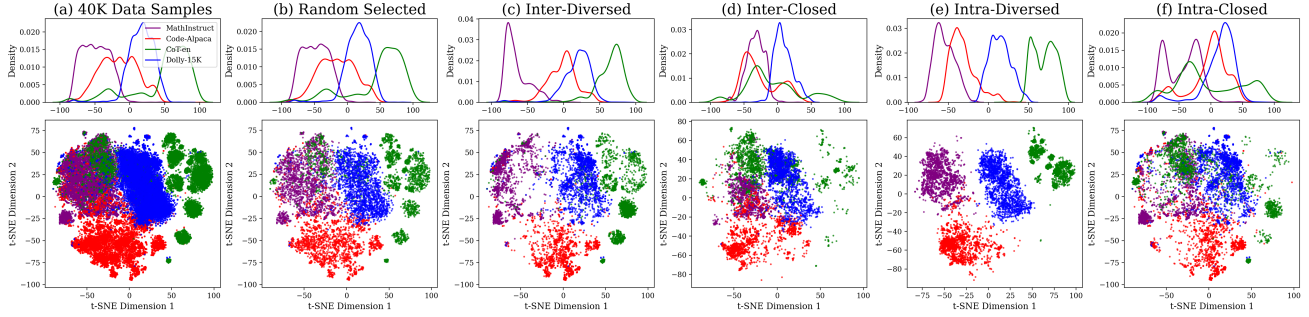


Figure 1. The t-SNE visualization of embeddings for data samples with different distributions on Qwen2-7B. (a) The data pool of all 40,000 samples, (b) Randomly selected subset, (c) Distribution of data farthest from other domain centroids based on Inter-Diversity, (d) Distribution of data closest to other domain centroids based on Inter-Diversity, (e) Distribution of data closest to its own domain centroid based on Inter-Diversity, (f) Distribution of data farthest from its own domain centroid based on Inter-Diversity.

ture into the LLM to be tuned, acting as a trainable probe module conditioned on the inherent knowledge and weights of the given LLM. The probe module takes semantic entropy as a proxy measure of diversity, and output reward scores, and select suitable data subsets aligned with the LLM’s underlying mixture distributions for better diversity. This is achieved by training the probe module on synthetically generated domain-aware data by the model itself, and using the data after selection to further self-fine-tuning. Extensive experiments on various state-of-the-art (SOTA) LLMs like the Qwen and LLaMA series verify the effectiveness of **DAAR** in enhancing overall model capabilities over many SOTA baseline methods.

Our contributions are threefold:

- We empirically and theoretically demonstrate how data plays a crucial role to enhance LLMs in semantic diversity, providing generalized modeling based on mixture of component models.
- We propose a lightweight, self-rewarding method for selecting data in domain-undetermined scenarios, which utilizes synthesized model-aware data to maximize domain diversity and fine-tuning performance.
- We verify that the proposed methods can effectively balance seven diverse benchmarks for improved overall performance when applied to representative LLMs, whereas other SOTA methods struggle in such challenging scenarios. Our code is open-sourced<sup>1</sup> to foster more in-depth understanding and future progress.

## 2. Related Work

**Data Selection** Fine-tuning is a pivotal training paradigm for enhancing LLMs’ task-specific and domain-specific ca-

pabilities. Research has shown that a small set of instruction pairs can enable LLMs to follow major instructions effectively (Zhou et al., 2024; Chen et al., 2024a). This fine-tuning can be achieved through rule-based methods, which focus on attributes such as Error L2-Norm (Paul et al., 2021) and token length (Raffel et al., 2020). More recently, model-based heuristics have been explored, including methods based on instruction-following difficulty (Li et al., 2024a), GPT scoring (Chen et al., 2024d; Wettig et al., 2024), data model selection (Engstrom, 2024), and influence scores derived from loss (Xia et al., 2024).

**Diversity & Data Mixing** A fundamental principle for LLMs is being able to handle diverse human requests, underscoring data diversity as essential for effective fine-tuning (Yu et al., 2022; Ding et al., 2023). Data diversity encompasses aspects such as data deduplication (Abbas et al., 2023), the coverage scope of tags (Lu et al., 2024), model-based diversity evaluation (Liu et al., 2024b; Zhang et al., 2024), and scaling properties (Song et al., 2024). Typically, data mixing approaches (Albalak et al., 2023; Ye et al., 2024; Ge et al., 2024) focus on adjusting the proportional weights of different domains to enhance model capabilities.

**Our Position** From a modeling perspective, our work shares a focus with many data mixing methodologies regarding diversity measurement. However, we address a more challenging setting relevant to real-world applications, where available datasets often lack domain labels. This situation presents challenges for existing mixing methods in balancing label granularity and normalization, and in determining which domains should be considered as candidates for improved solution spaces and tuning performance.

Methodologically, our approach aligns with the data selection category but differs in both the learning process (utilizing a rewarding model) and the selection criteria (employing

<sup>1</sup><https://github.com/modelscope/data-juicer/tree/DaaR>

semantic entropy). Additionally, we revisit the applicability of existing selection methods in multi-domain scenarios. This area is under-explored and requires new insights to avoid biased modeling of diverse domain distributions—a topic we further investigate in this paper.

### 3. Motivational Observations

In this section, we will explore how data with different domain-specific diversity affects model capabilities through experimental data pools, featuring contrastive data distributions in terms of inter-domain and intra-domain diversity.

#### 3.1. Seed Data Pools and Basic Setting

**Data Pools and Sources** To explore how selecting data samples from extensive and diverse data repositories affects the foundational capabilities of LLMs, we construct various data pools and consistently fine-tune LLMs on them. We then analyze the performance changes and attribute these changes to the different controlled data pools.

The seed data pool is sourced from following datasets: Dolly-15k (Conover et al., 2023) for common sense, Coten (Chung et al., 2024) for reasoning, Math-Instruct (Yue et al., 2024) for mathematics, and Code-Alpaca (Chaudhary, 2023) for coding. Each dataset was randomly tailored to 10,000 entries, resulting in a combined data pool of 40,000 entries. Following instruction tuning practices (Zhou et al., 2024; Liu et al., 2024b), we then uniformly sample 8,000 data entries as a referenced data pool for random baseline. In subsequent sections, we will introduce how to construct other comparative pools with the same size to random pool.

**Benchmarks** Aligned with representative capabilities of leading open-source LLMs, we select the following widely used evaluation sets: NQ (Kwiatkowski et al., 2019) and TriviaQA (Joshi et al., 2017) for common sense, Hellaswag (Zellers et al., 2019) for reasoning, GSM8K (Cobbe et al., 2021) and MATH (Hendrycks et al., 2021) for mathematics, MBPP (Austin et al., 2021) and HumanEval (Chen et al., 2021) for coding. To evaluate the comprehensive performance of LLMs across domains, we employ the average metric (AVG) as the primary evaluation criterion.

**Models & Implementation** To ensure the effectiveness and applicability of our empirical findings, we employ the Qwen2 series (Qwen2-7B & Qwen2.5-7B) (Yang et al., 2024) and the Llama3.1-8B (Dubey et al., 2024) as representative SOTA base models to be fine-tuned. All experiments are conducted under identical training and evaluation protocols with two independent repetitions. Full platform, training and evaluation details are provided in Appendix B.

### 3.2. Data Pools with Contrastive Distributions

To systematically analyze the impact of domain-specific diversity patterns on model capabilities, we propose a contrastive construction with three phases: (A) Foundational Definitions, (B) Diversity Metric Formulation, and (C) Distribution Synthesis.

**(A) Foundational Definitions** Let the composite dataset  $\mathcal{D} = \bigcup_{k=1}^K \mathcal{D}_k$  comprise  $K = 4$  distinct domains, where each domain subset  $\mathcal{D}_k$  contains  $N_k = |\mathcal{D}_k|$  samples. We represent each data instance through its semantic embedding  $\mathbf{x}_i^{(k)} \in \mathbb{R}^d$  extracted from the **Embedding** layer of the pre-trained LLM, capturing high-dimensional semantic features. The domain centroid  $\mathcal{C}_k$  serves as the semantic prototype:

$$\mathcal{C}_k = \frac{1}{N_k} \sum_{i=1}^{N_k} \mathbf{x}_i^{(k)}. \quad (1)$$

This centroid-based representation enables geometric interpretation of domain characteristics in the embedding space. We dissect data diversity into two complementary aspects:

**(B.1) Inter-Diversity** It quantifies the diversity between distinct domains through centroid geometry. For sample  $\mathbf{x}_i^{(k)}$ , its cross-domain similarity is measured by:

$$\phi_{\text{inter}}(\mathbf{x}_i^{(k)}) = \sum_{\substack{j=1 \\ j \neq k}}^K \frac{\mathbf{x}_i^{(k)} \cdot \mathcal{C}_j}{\|\mathbf{x}_i^{(k)}\| \|\mathcal{C}_j\|}. \quad (2)$$

The global inter-diversity metric  $\Phi_{\text{inter}}$  computes the expected pairwise centroid distance:

$$\Phi_{\text{inter}} = \mathbb{E}_{k \neq l} [\|\mathcal{C}_k - \mathcal{C}_l\|_2] = \frac{1}{\binom{K}{2}} \sum_{k=1}^{K-1} \sum_{l=k+1}^K \|\mathcal{C}_k - \mathcal{C}_l\|_2. \quad (3)$$

This formulation reflects a key insight: maximizing  $\Phi_{\text{inter}}$  encourages domain separation, while minimization leads to overlapping representations. Fig. 1 demonstrates this continuum through t-SNE projections – high  $\Phi_{\text{inter}}$  manifests as distinct cluster separation with clear margins (Fig. 1.(c)), whereas low values produce entangled distributions (Fig. 1.(d)). Full analysis is detailed in Appendix D.1.

**(B.2) Intra-Diversity** Focusing solely on the separation between different domains may hinder the model’s ability to learn the knowledge specific to a given domain. Hence we measure variation within each domain. We calculate sample similarity to its domain center:

$$\phi_{\text{intra}}(\mathbf{x}_i^{(k)}) = \frac{\mathbf{x}_i^{(k)} \cdot \mathcal{C}_k}{\|\mathbf{x}_i^{(k)}\| \|\mathcal{C}_k\|}. \quad (4)$$

And the domain-level variance metric is defined as:

$$\Phi_{\text{intra}}^{(k)} = \frac{1}{N_k} \sum_{i=1}^{N_k} \|\mathbf{x}_i^{(k)} - \mathcal{C}_k\|_2^2. \quad (5)$$

Controlled manipulation of  $\Phi_{\text{intra}}$  reveals critical trade-offs: lower variance (tight clusters near  $\mathcal{C}_k$ ) enhances domain-specific feature learning but risks over-specialization. Higher variance improves robustness at the cost of potential cross-domain interference. The visualization in Fig. 1 (e-f) illustrates this scenario that concentrated distributions exhibit sharp marginal peaks, while dispersed variants show overlapping density regions.

**(C) Distribution Synthesis** For each domain  $\mathcal{D}_k$ , we compute sample-wise diversity scores  $\{\phi_{\text{inter}}(\mathbf{x}_i^{(k)})\}_{i=1}^{N_k}$  and  $\{\phi_{\text{intra}}(\mathbf{x}_i^{(k)})\}_{i=1}^{N_k}$ . The construction proceeds via partition each  $\mathcal{D}_k$  into 20% intervals based on the percentiles of  $\phi_{\text{inter}}$  for **inter-diversity control**, and partition the  $\phi_{\text{intra}}$  scores into 20% quantile intervals for **intra-diversity control**.

The 20% interval results in five choices of data selection per domain, parameterizing the trade-off between diversity preservation and domain specificity. As demonstrated in Appendix D.2 (Fig. 10 and Fig. 11), this quantization process induces measurable distribution shifts.

### 3.3. Experimental Observations

Table 1 presents comprehensive evaluations across seven benchmarks, where the notation *Inter-Diversity (X-Y)* indicates samples ranked in the top (100-Y)% to (100-X)% of cross-domain similarity scores. Due to space constraints, we present only the results for the top 20%, middle 20%, and bottom 20%. More results can be found in Appendix D.7.

**Diversity-Aware Performance:** Our diversity-controlled selections reveal two critical observations:

- **Varied Improvement Patterns:** Both models demonstrate marked improvements over RAW distributions across all diversity conditions, but the effects of their improvements vary. For Llama3.1-8B, *Inter-D* (80-100) achieves 38.98 average accuracy (+3.12 over RAW), outperforming the RANDOM baseline by 1.71, while *Inter-D* (0-20) is below RANDOM of 0.09.
- **Model-dependent Performance Peak:** Each model exhibits distinct optimal operating points along the diversity spectrum. Llama3.1-8B reaches peak performance at *Inter-D* (80-100) and *Intra-D* (80-100), suggesting complementary benefits from both diversity types. Qwen2-7B peaks in inter-type selection at low inter-diversity, while it peaks in intra-type selection at high intra-diversity.

These results show the promising potential of diversity-aware data selection, motivating us to further understand the performance variance more formally and propose principled solutions to adaptively achieve the performance peaks.

**Practical Challenges** Despite existing positive improvements on overall performance, the optimal distribution parameters exhibit model-dependent variability. This parameter sensitivity suggests the existence of *multiple local optima* in the diversity-performance landscape. Two constraints merit consideration for real-world applications.

**(1) Label Dependency:** The studied heuristic strategies *Inter-Diversity* and *Intra-Diversity* currently require domain-labeled data for centroid calculation. **(2) Distribution Transiency:** The optimal diversity parameters (e.g., 80-100 vs. 40-60) show sensitivity across tasks and models, necessitating automated and potentially costly configuration search.

## 4. Theoretical Analysis and Insights

In this section, we first formalize the optimization dynamics of multi-domain data aggregation for enhancing LLMs' comprehensive capabilities. Building on the empirical observations from Sec. 3, we then establish theoretical connections between distributional diversity and emergent model behaviors. Finally, we demonstrate the fundamental limitation of explicit diversity optimization in undetermined-domain scenarios.

### 4.1. Ideal Optimization Formulation

During the training process of LLMs, various sources of labeled data are often collected to enhance models' capabilities across multiple dimensions. Let  $\mathcal{K} = \{1, \dots, K\}$  represent the set of labeled domains, where  $K$  is determined by real-world task requirements (e.g.,  $K = 4$  in our experiments). For each domain  $k \in \mathcal{K}$ , data samples  $\mathbf{x}_i^{(k)} \in \mathcal{D}_k$  are generated according to a distribution  $\mathcal{D}_k$ . The data distributions are assumed mutually distinct across different domains, leading to an ideal **I.I.D. per-domain hypothesis**: each domain  $k$  corresponds to an independent model  $h_k \in \mathcal{H}$ . The standard optimization goal thus can be:

$$\forall k \in \mathcal{K}, \quad \min_{h_k \in \mathcal{H}} \mathcal{L}_{\mathcal{D}_k}(h_k), \quad (6)$$

where  $\mathcal{L}_{\mathcal{D}_k}(h_k) = \mathbb{E}_{(x,y) \sim \mathcal{D}_k} [l(h_k(x), y)]$  is the empirical risk given a specific loss function  $l$ .

**Counterintuitive Findings** If the distributions  $\{\mathcal{D}_k\}_{k=1}^K$  are strictly I.I.D., the risk  $\mathcal{L}_{\mathcal{D}_k}(h_k)$  should depend only on  $\mathcal{D}_k$ . However, numerous previous studies (Zhao et al., 2024a; Tirumala et al., 2023) have demonstrated the presence of synergistic and antagonistic effects between different datasets. This is further demonstrated in Sec. 3 (Fig. 1)

Table 1. Performance of Llama3.1-8B and Qwen2-7B on various downstream task benchmarks under different constructed Inter-Diversity (Inter-D) and Intra-Diversity (Intra-D) distributions.

Models	Distribution	Common Sense		Reasoning		Mathematics		Coding		Avg
		NQ	TriviaQA	Hellaswag	GSM8K	MATH	MBPP	HumanEval		
Llama3.1-8B	<b>RAW</b>	14.13	65.90	74.62	54.80	7.90	5.00	28.66	35.86	
	<b>RANDOM</b>	21.99	64.83	74.72	55.70	14.50	5.10	24.09	37.27	
	Inter-D (0-20)	19.28	65.79	74.44	54.90	6.50	4.30	35.06	37.18	
	Inter-D (40-60)	23.70	65.14	74.86	56.40	17.15	5.00	24.40	38.09	
	<b>Inter-D (80-100)</b>	23.76	64.43	75.20	56.40	15.05	4.50	33.54	<b>38.98</b>	
	Intra-D (0-20)	22.08	65.08	75.00	54.70	16.20	4.40	33.54	38.71	
	Intra-D (40-60)	22.12	64.74	74.87	54.00	16.00	6.00	27.44	37.88	
	<b>Intra-D (80-100)</b>	19.78	64.77	74.51	56.50	13.00	5.20	37.50	<b>38.75</b>	
Qwen2-7B	<b>RAW</b>	8.03	59.58	73.00	78.00	5.70	5.00	60.98	41.47	
	<b>RANDOM</b>	13.28	58.27	73.00	75.35	35.36	52.20	63.72	53.02	
	<b>Inter-D (0-20)</b>	15.18	59.28	73.34	74.50	34.94	53.10	68.60	<b>54.13</b>	
	Inter-D (40-60)	14.62	58.58	73.35	72.50	34.50	52.50	61.28	52.47	
	Inter-D (80-100)	9.30	57.72	73.14	74.60	28.00	51.30	63.42	51.07	
	Intra-D (0-20)	12.64	58.54	73.35	75.10	8.75	51.10	61.59	48.72	
	Intra-D (40-60)	15.24	58.57	73.12	74.70	32.50	51.80	64.02	52.85	
	<b>Intra-D (80-100)</b>	11.91	57.88	73.29	75.00	36.05	52.50	66.16	<b>53.25</b>	

that certain domain mixtures lead to catastrophic performance degradation (e.g. *Intra-D (0-20)* in MATH with Qwen2). This contradicts the above I.I.D. hypothesis, suggesting that the simplified and conventional formulation in Eq (6) fails to capture cross-domain interference.

#### 4.2. Introducing Mixture of Underlying Distributions

Inspired by the counterintuitive findings, we posit that each domain distribution  $\mathcal{D}_k$  arises from the mixture of  $M$  latent distributions  $\{\tilde{\mathcal{D}}_m\}_{m=1}^M$  representing foundational LLM capabilities ( $M \ll K$  in practice). This leads to our core statistical assumption:

**Assumption 4.1** (Latent Capability Structure). For each observed domain  $k \in \mathcal{K}$ , its data distribution decomposes into  $M$  latent capability distributions:

$$\mathcal{D}_k = \sum_{m=1}^M \pi_{km} \tilde{\mathcal{D}}_m, \quad \sum_{m=1}^M \pi_{km} = 1, \quad (7)$$

where  $\tilde{\mathcal{D}}_m$  indicates the  $m$ -th foundational capability. The weights  $\pi_{km}$  reflect domain-specific capability composition.

To analyze how data optimization interacts with latent capability distributions, we further posit that each foundational capability admits an optimal configuration:

**Assumption 4.2** (Capability Optimality). Each foundational capability admits a unique optimal predictor:

$$\exists h_{\theta_m^*} \in \mathcal{H} \text{ s.t. } \theta_m^* = \operatorname{argmin}_{\theta} \mathbb{E}_{(x,y) \sim \tilde{\mathcal{D}}_m} [l(h_{\theta}(x), y)]. \quad (8)$$

The loss  $l$  is strongly convex, holding for cross-entropy or MSE, where  $h_{\theta_m}$ , termed the component model, represents a model's manifestation of specific foundational capabilities.

This leads to our key result formalizing how real-world training data activates latent capabilities via component models:

**Proposition 4.3.** Under Assumption 4.1-4.2, the minimizer of the cross-domain average risk

$$\min_{\{\theta_m\}} \mathbb{E}_{k \sim \mathcal{K}} \left[ \mathcal{L}_{\mathcal{D}_k} \left( \sum_{m=1}^M \pi_{km} h_{\theta_m} \right) \right] \quad (9)$$

admits a solution  $\{\theta_m^*\}_{m=1}^M$  where each  $h_{\theta_m^*}$  optimizes the corresponding foundational capability  $\tilde{\mathcal{D}}_m$ .

**Remark** Proposition 4.3 reveals an underlying fact: optimal or suboptimal solutions can be achieved through data selection to enhance the overall model performance. This is further validated by the role of the coefficients  $\pi_{km}$ , which act as *capability selectors* to configure domain-specific behavior, demonstrating the impact of data composition.

#### 4.3. Diversity Influence on the Optimization

Building upon Proposition 4.3, we analyze the intrinsic relationship between diversity and capability composition. The mixture coefficients  $\pi_{km}$  inherently govern both inter- and intra-domain diversity formulated in Sec. 3.2, differing in their geometric properties in the latent capability space.

**Centroids with Coefficients** Let  $\mathcal{C}_m \in \mathbb{R}^d$  denote the centroid vector of latent capability  $\tilde{\mathcal{D}}_m$  in the embedding space. The domain centroid  $\mathcal{C}_k$  can be expressed as:

$$\mathcal{C}_k = \sum_{m=1}^M \pi_{km} \mathcal{C}_m. \quad (10)$$

This linear combination implies that the inter- and intra-diversity are determined by  $\pi_{km}$  configurations:

**Proposition 4.4** (Diversity Decomposition). *The inter-diversity metric decomposes into:*

$$\Phi_{inter} = \sum_{m=1}^M \sum_{n=1}^M \lambda_m \lambda_n \|\mathcal{C}_m - \mathcal{C}_n\|_2, \quad (11)$$

where  $\lambda_m = \mathbb{E}_k[\pi_{km}]$ . And the intra-diversity satisfies:

$$\Phi_{intra}^{(k)} \leq \sum_{m=1}^M \pi_{km} \|\mathcal{C}_m - \mathcal{C}_k\|_2^2 + \mathbb{E}_{m \sim \pi_k} [\text{Var}(\tilde{\mathcal{D}}_m)]. \quad (12)$$

The inter-diversity result follows from substituting  $\mathcal{C}_k = \sum \pi_{km} \mathcal{C}_m$  into  $\mathbb{E}_{k \neq l} \|\mathcal{C}_k - \mathcal{C}_l\|$  and applying Jensen's inequality. The intra-diversity bound combines the variance decomposition within each latent capability. Full proof is provided in Appendix C.2.

#### 4.4. Theoretical Insights

Collectively, results in this section provide a unified framework to explain the varied patterns and existence of peak performance observed in Sec. 3.3, providing theoretical insights and guidance for designing our following algorithm dealing with undetermined data.

**Diversity's Influence on LLMs' Capability:** Based on Proposition 4.4, we conjecture that the Inter-/Intra-Diversity, which can be explicitly modeled by  $\pi$ , also governs  $\pi$ -variation control for component model mixing and thus the final overall performance. Proposition 4.3 further suggests that improper diversity levels may induce model suboptimality by constraining overall capability, consistent with the distribution-dependent empirical results in Sec. 3.

**Robust Diversity Selection Strategies:** Based on Proposition 4.4, it can be observed that averaging the  $\pi_{km}$  helps to mitigate the missing of underlying optimal predictor  $\theta_m^*$ . From this view, the random baseline can gain relatively stable improvements in expectation. A more robust yet simple strategy can be derived: ensemble across candidate models trained on multiple data pools with distribution-varied inter- and intra-diversity, e.g., via techniques like voting or model weights averaging. This can be corroborated by results in Table 1, such as the case for Llama3.1-8B.

**Challenges in Undetermined-Domain Scenarios:** However, all the selection strategies discussed so far face intractable solutions in undetermined domains with explicit domain labels, as Proposition 4.4 technically revealed: (1) ambiguous domain boundaries, e.g., blended instruction types; (2) partial overlaps in latent capabilities; and (3) absence of centroid priors  $\{\mathcal{C}_m\}$ . These intrinsic constraints motivate our *model-aware diversity reward* in the following Sec. 5, which harnesses domain-diversity awareness into reward modeling without requiring explicit parameterization for such structural assumptions.

## 5. DAAR: Diversity as a Reward

To address the challenges identified and leverage the insights gained in previous Sec. 3 and Sec. 4, we establish a data selection method **DAAR** guided by diversity-aware reward signals. It comprises three key components illustrated in subsequent sections: (1) model-aware centroid synthesis, (2) two-stage training with reward probe, and (3) diversity-driven data selection.

### 5.1. Model-Aware Training Data

**Model-Aware Centroid Construction** The proposed method initiates with centroid self-synthesis through a two-phase generation process to address two fundamental challenges: (1) eliminating dependency on human annotations through automated domain prototyping, and (2) capturing the base model's intrinsic feature space geometry for model-aware domain separation.

- **Phase 1 - Seed Generation:** For each domain  $k$ , generate 5 seed samples  $\mathcal{S}_k^{(0)}$  via zero-shot prompting with domain-specific description templates, establishing initial semantic anchors. The prompt details and ablation of choices on sample number are provided in Appendix B.7.
- **Phase 2 - Diversity Augmentation:** Iteratively expand  $\mathcal{S}_k^{(t)}$  through context-aware generation, conditioned on a sliding window buffer with 3 random anchors sampled from the  $(t-1)$  iteration  $\mathcal{S}_k^{(t-1)}$ . The generated sample  $\mathbf{x}'$  will be admitted during the iteration via geometric rejection sampling:

$$\max_{\mathbf{x} \in \mathcal{S}_k^{(t-1)}} \cos(\mathcal{M}_{\text{ebd}}(\mathbf{x}'), \mathcal{M}_{\text{ebd}}(\mathbf{x})) < \tau = 0.85, \quad (13)$$

where  $\mathcal{M}_{\text{ebd}}(\cdot)$  indicates the embedding layer outputs of the given LLM. This process terminates when  $|\mathcal{S}_k| = 30$ . More analysis and ablation on these choices are provided in the Appendix. In Appendix D.3, we found that the adopted number of samples sufficiently leads to a stable convergence and larger data quantity does not impact the final centroids. In Appendix D.4, we found that this synthetic data has the ability to produce domain-representative data with clear distinction. Interestingly, the generated content consistently exhibits the greatest divergence between common sense, reasoning, and coding domains across model architectures and parameters.

The domain centroid is then computed from the final augmented set  $\mathcal{S}_k$  using the model's knowledge prior:

$$\mathcal{C}_k = \frac{1}{|\mathcal{S}_k|} \sum_{\mathbf{x}_i \in \mathcal{S}_k} \mathcal{M}_{\text{ebd}}(\mathbf{x}_i). \quad (14)$$

This captures the LLM's intrinsic feature space geometry while eliminating dependency on human annotations.

**Domain-Aware Clustering** We then automatically construct pseudo-labels for the given data samples based on the previously synthesized centroids  $\{C_k\}_{k=1}^K$ . Take them as fixed prototypes, we perform constrained k-means clustering in the embedding space:

$$\arg \min_{\{S_k\}} \sum_{k=1}^K \sum_{\tilde{x} \in S_k} \|\mathcal{M}_{\text{ebd}}(\tilde{x}) - C_k\|^2. \quad (15)$$

This produces the seed dataset  $\mathcal{D}_{\text{probe}}$  containing pseudo-labels  $\{\tilde{y}_i\}_{i=1}^n$  where  $\tilde{y}_i \in \{1, \dots, K\}$ , with model-induced and embedding-derived domain label assignments.

## 5.2. Training for Self-Rewarding Abilities

**Stage 1: Domain Discrimination** The proposed **DAAR** then establishes model-aware domain discrimination abilities through a multi-layer perceptron (MLP) probe module,  $\psi_{\text{dom}}$ , attached to the layer-3 of the LLMs  $\mathcal{M}_3(\tilde{x})$ . The probe will be trained meanwhile all the parameters of the LLM are frozen. This achieves a preferable balance between effectiveness and cost, with detailed analysis regarding the choice of Layer-3 presented in Appendix D.5. Specifically, with pseudo-label  $\tilde{y}$ , we can compute domain probabilities as:

$$p_k(\tilde{x}) = \text{softmax}(\psi_{\text{dom}}(\mathcal{M}_3(\tilde{x}))), \quad \psi_{\text{dom}} : \mathbb{R}^d \rightarrow \mathbb{R}^K, \quad (16)$$

where  $\psi_{\text{dom}}$  is optimized via cross-entropy loss function:

$$\mathcal{L}_{\text{dom}} = -\frac{1}{|\mathcal{D}_{\text{probe}}|} \sum_{(\tilde{x}, \tilde{y}) \in \mathcal{D}_{\text{probe}}} \sum_{k=1}^K \mathbb{I}_{[k=\tilde{y}]} \log p_k(\tilde{x}), \quad (17)$$

where  $\mathbb{I}_{[k=\tilde{y}]}$  denotes the indicator function. We employ single-sample batches with the AdamW optimizer to prevent gradient averaging across domains. Training consistently converges and achieves 92.7% validation accuracy on domain classification, as shown in Fig. 2 (a).

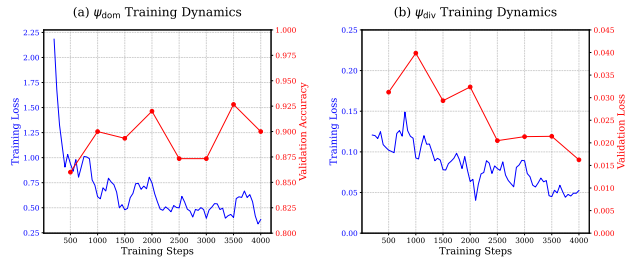


Figure 2. Training loss and validation process of the two stages of **DAAR** on Qwen2-7B, detailed results are in Appendix D.6.

**Stage 2: Diversity Rewarding** Building on the stabilized domain probe module, we quantify sample-level diversity

through predictive entropy:

$$H(\tilde{x}) = - \sum_{k=1}^K p_k(\tilde{x}) \log p_k(\tilde{x}). \quad (18)$$

To enable efficient reward computation during data selection, we then train another 5-layer MLP  $\psi_{\text{div}}$  to directly estimate  $H(\tilde{x})$  from  $\mathcal{M}_3(\tilde{x})$ :

$$\hat{H}(\tilde{x}) = \psi_{\text{div}}(\mathcal{M}_3(\tilde{x})), \quad \psi_{\text{div}} : \mathbb{R}^d \rightarrow \mathbb{R}^+. \quad (19)$$

This diversity probe module  $\psi_{\text{div}}$  shares  $\psi_{\text{dom}}$ 's architecture up to its final layer (replaced with single-output regression head), trained using entropy-scaled MSE:

$$\mathcal{L}_{\text{div}} = \frac{1}{|\mathcal{D}_{\text{probe}}|} \sum_{\tilde{x} \in \mathcal{D}_{\text{probe}}} \left( \hat{H}(\tilde{x}) - H(\tilde{x}) \right)^2. \quad (20)$$

This module is also well-converged as shown in Fig. 2 (b).

**Data Selection:** After training the module  $\psi_{\text{div}}$ , we can use its output to select data samples. Building on the theoretical insights in Sec. 4.4, data points that are closer to other centroids and more dispersed within their own centroid are more beneficial for enhancing the comprehensive capabilities of the model. Therefore, we use the predicted entropy-diversity score as a reward, selecting the top 20% with the highest scores as the final data subset for fine-tuning.

## 5.3. Empirical Validation and Main Results

To validate the efficacy of **DAAR**, we conduct experiments comparing more SOTA methods on the data pools in Sec. 3.1 with critical modifications: all domain-specific labels are deliberately stripped. This constraint mimics more challenging real-world scenarios and precludes direct comparison with data mixture methods requiring domain label prior.

**Baselines** We use the following data selection methods for comprehensive evaluation: (1) RANDOM SELECTION: traditional random sampling; (2) INSTRUCTION LEN: measuring instruction complexity by token count (Cao et al., 2023); (3) ALPAGASUS (Chen et al., 2024d): using ChatGPT for direct quality scoring of instruction pairs; (4-5) INSTAG (Lu et al., 2024): semantic analysis approach with INSTAG-C (complexity scoring via tag quantity) and INSTAG-D (diversity measurement through tag set expansion); (6) SUPERFILTER (Li et al., 2024a): response-loss-based complexity estimation using compact models; (7-9) DEITA (Liu et al., 2024b): model-driven evaluation with DEITA-C (complexity scoring), DEITA-Q (quality scoring), and DEITA-D (diversity-aware selection). Detailed configurations for these baselines are in Appendix B.4.

### 5.3.1. OVERALL PERFORMANCE

The experimental results are presented in Table 2, where INSTAG-BEST and DEITA-BEST represent the optimal vari-

Table 2. Evaluation results of Llama3.1-8B, Qwen2-7B, and Qwen2.5-7B across various downstream task benchmarks. **DAAR** demonstrates superiority in average performance (AVG) compared to other baselines.

Models	Distribution	Common Sense		Reasoning		Mathematics		Coding		Avg
		NQ	TriviaQA	Hellaswag	GSM8K	MATH	MBPP	HumanEval		
Llama3.1-8B	<b>RAW</b>	14.13	65.90	74.62	54.80	7.90	5.00	28.66	35.86	
	<b>RANDOM</b>	21.99	64.83	74.72	55.70	14.50	5.10	24.09	37.27	
	<b>INSTRUCTION LEN</b>	15.34	63.60	73.73	54.00	15.40	3.60	30.80	36.64	
	<b>ALPAGASUS (Chen et al., 2024d)</b>	21.57	64.37	74.87	55.20	17.65	4.60	16.16	36.34	
	<b>INSTAG-BEST (Lu et al., 2024)</b>	18.12	64.96	74.01	55.70	15.50	4.80	37.81	38.70	
	<b>SUPERFILTER (Li et al., 2024a)</b>	22.95	64.99	76.39	57.60	6.05	2.60	40.55	38.73	
	<b>DEITA-BEST (Liu et al., 2024b)</b>	15.58	64.97	74.21	55.00	13.05	4.60	34.46	37.41	
	<b>DAAR (Ours)</b>	20.08	64.55	74.88	54.8	15.30	4.70	37.50	<b>38.83</b>	
Qwen2-7B	<b>RAW</b>	8.03	59.58	73.00	78.00	5.70	5.00	60.98	41.47	
	<b>RANDOM</b>	13.28	58.27	73.00	75.35	35.36	52.20	63.72	<b>53.02</b>	
	<b>INSTRUCTION LEN</b>	8.62	58.44	72.86	73.30	27.05	53.10	63.72	51.01	
	<b>ALPAGASUS (Chen et al., 2024d)</b>	13.67	57.94	73.04	73.90	32.30	51.40	63.41	52.24	
	<b>INSTAG-BEST (Lu et al., 2024)</b>	9.51	58.50	73.06	74.70	35.35	51.90	64.70	52.53	
	<b>SUPERFILTER (Li et al., 2024a)</b>	19.16	58.98	72.99	73.70	30.10	52.40	58.85	52.31	
	<b>DEITA-BEST (Liu et al., 2024b)</b>	16.41	57.80	72.70	76.10	29.05	52.40	64.63	52.73	
	<b>DAAR (Ours)</b>	16.88	57.58	73.03	75.40	38.1	52.00	64.94	<b>53.99</b>	
Qwen2.5-7B	<b>RAW</b>	8.84	58.14	72.75	78.20	9.10	7.40	78.05	44.64	
	<b>RANDOM</b>	11.46	57.85	73.08	78.90	13.15	62.50	71.65	<b>52.65</b>	
	<b>INSTRUCTION LEN</b>	11.34	58.01	72.79	78.00	15.80	62.30	68.12	52.34	
	<b>ALPAGASUS (Chen et al., 2024d)</b>	10.40	57.87	72.92	77.20	18.75	61.80	65.55	52.07	
	<b>INSTAG-BEST (Lu et al., 2024)</b>	11.08	58.40	72.79	76.40	16.40	62.90	70.43	52.63	
	<b>SUPERFILTER (Li et al., 2024a)</b>	13.54	58.51	72.89	79.30	11.35	39.50	65.25	48.62	
	<b>DEITA-BEST (Liu et al., 2024b)</b>	10.50	58.17	73.14	74.60	16.60	62.00	72.26	52.47	
	<b>DAAR (Ours)</b>	15.83	58.65	72.48	80.20	16.70	64.20	68.29	<b>53.76</b>	

ants from their respective method families. Our experiments clearly demonstrate the effectiveness of **DAAR** across three major language models and seven challenging benchmarks. A detailed analysis is provided below.

**High-Difficulty Scenario:** The task of balanced capability enhancement proves particularly challenging for existing methods. While some baselines achieve strong performance on specific tasks (e.g., SuperFilter’s 40.55 on HumanEval for Llama3.1), they suffer from catastrophic performance drops in other domains (e.g., SuperFilter’s 6.05 on MATH). Only three baseline methods perform better than RANDOM selection, with notably severe degradation applied in Qwen-series models, all of which fall below the RANDOM performance. We hypothesize this stems from *over-specialization* – excessive focus on narrow capability peaks at the expense of broad competence (visualized in Appendix B.5). Our method’s robustness stems from preventing extreme distribution shifts through diversity constraints.

**Universal Superiority:** **DAAR** establishes new SOTA averages across all models, surpassing the best baselines by **+0.14** (Llama3.1), **+0.97** (Qwen2), and **+1.11** (Qwen2.5).

The proposed method uniquely achieves *dual optimization* in critical capabilities: **Mathematical Reasoning:** Scores 38.1 MATH (Qwen2) and 16.70 MATH (Qwen2.5), with 7.4% and 27.0% higher than respective random baselines.

**Coding Proficiency:** Maintains 64.94 HumanEval (Qwen2)

and 64.20 MBPP (Qwen2.5) accuracy with <1% degradation from peak performance. This demonstrates **DAAR**’s ability to enhance challenging STEM capabilities while preserving core competencies, a critical advancement over specialized but unstable baselines.

**Cost-Efficiency and Flexibility:** Compared to baseline methods requiring GPT-based evaluators (ALPAGASUS, INSTAG) or full LLaMA-7B inference (DEITA), **DAAR** achieves superior efficiency through data-model co-optimizations. Our method makes the LLM ability of self-rewarding from dedicated data synthesis, and operates on frozen embeddings from layer 3 (vs. full 32-layer inference in comparable methods), reducing computational overhead while maintaining capability integrity. The lightweight 5-layer MLP probe module requires only 9GB GPU memory during training (vs. 18~24GB for LLM-based evaluators) and adds merely 76M parameters. This plug-and-play feature enables seamless integration of **DAAR** with existing LLMs without additional dependency management.

## 6. Conclusion and Future Work

In this paper, we propose a new approach to fine-tuning LLMs with data that lacks clear domain labels, using diversity as a guiding principle. Our method allows LLMs to automatically select and benefit from diverse datasets. By

measuring semantic diversity with entropy, we employ a self-reward mechanism built upon the given LLM, identifying data that best fits the model’s natural tendencies in terms of its underlying knowledge distribution. Our experiments with various SOTA LLMs show notable superiority of the method over SOTA methods, highlighting the potential of data diversity to enhance model overall performance.

This research demonstrates feasibility of reward modeling on LLM data diversity and deepens the understanding of its utilities, especially when domain labels are missing or uncertain. Future work could include developing methods to efficiently adjust diversity measures and learning algorithm, thus supporting LLMs in self-evolving towards artificial general intelligence in dynamic environments.

## References

Abbas, A. K. M., Tirumala, K., Simig, D., Ganguli, S., and Morcos, A. S. Semdedup: Data-efficient learning at web-scale through semantic deduplication. In *ICLR 2023 Workshop on Mathematical and Empirical Understanding of Foundation Models*, 2023.

Achiam, J., Adler, S., Agarwal, S., Ahmad, L., Akkaya, I., Aleman, F. L., Almeida, D., Altenschmidt, J., Altman, S., Anadkat, S., et al. Gpt-4 technical report. *arXiv preprint arXiv:2303.08774*, 2023.

Albalak, A., Pan, L., Raffel, C., and Wang, W. Y. Efficient online data mixing for language model pre-training. In *RoFoMo: Robustness of Few-shot and Zero-shot Learning in Large Foundation Models*, 2023.

Austin, J., Odena, A., Nye, M., Bosma, M., Michalewski, H., Dohan, D., Jiang, E., Cai, C., Terry, M., Le, Q., et al. Program synthesis with large language models. *arXiv preprint arXiv:2108.07732*, 2021.

Cao, Y., Kang, Y., Wang, C., and Sun, L. Instruction mining: Instruction data selection for tuning large language models. *arXiv preprint arXiv:2307.06290*, 2023.

Chaudhary, S. Code alpaca: An instruction-following llama model for code generation. <https://github.com/sahil280114/codealpaca>, 2023.

Chen, D., Huang, Y., Ma, Z., Chen, H., Pan, X., Ge, C., Gao, D., Xie, Y., Liu, Z., Gao, J., Li, Y., Ding, B., and Zhou, J. Data-juicer: A one-stop data processing system for large language models. In *International Conference on Management of Data*, 2024a.

Chen, D., Huang, Y., Pan, X., Jiang, N., Wang, H., Ge, C., Chen, Y., Zhang, W., Ma, Z., Zhang, Y., Huang, J., Lin, W., Li, Y., Ding, B., and Zhou, J. Data-juicer 2.0: Cloud-scale adaptive data processing for foundation models, 2024b. URL <https://arxiv.org/abs/2501.14755>.

Chen, D., Wang, H., Huang, Y., Ge, C., Li, Y., Ding, B., and Zhou, J. Data-juicer sandbox: A comprehensive suite for multimodal data-model co-development, 2024c. URL <https://arxiv.org/abs/2407.11784>.

Chen, L., Li, S., Yan, J., Wang, H., Gunaratna, K., Yadav, V., Tang, Z., Srinivasan, V., Zhou, T., Huang, H., et al. Alpagasus: Training a better alpaca with fewer data. In *The Twelfth International Conference on Learning Representations*, 2024d.

Chen, M., Tworek, J., Jun, H., Yuan, Q., Pinto, H. P. D. O., Kaplan, J., Edwards, H., Burda, Y., Joseph, N., Brockman, G., et al. Evaluating large language models trained on code. *arXiv preprint arXiv:2107.03374*, 2021.

Chung, H. W., Hou, L., Longpre, S., Zoph, B., Tay, Y., Fedus, W., Li, Y., Wang, X., Dehghani, M., Brahma, S., et al. Scaling instruction-finetuned language models. *Journal of Machine Learning Research*, 25(70):1–53, 2024.

Cobbe, K., Kosaraju, V., Bavarian, M., Chen, M., Jun, H., Kaiser, L., Plappert, M., Tworek, J., Hilton, J., Nakano, R., et al. Training verifiers to solve math word problems. *arXiv preprint arXiv:2110.14168*, 2021.

Conover, M., Hayes, M., Mathur, A., Xie, J., Wan, J., Shah, S., Ghodsi, A., Wendell, P., Zaharia, M., and Xin, R. Free dolly: Introducing the world’s first truly open instruction-tuned llm, 2023.

Contributors, O. Opencompass: A universal evaluation platform for foundation models. *GitHub repository*, 2023.

Ding, N., Chen, Y., Xu, B., Qin, Y., Hu, S., Liu, Z., Sun, M., and Zhou, B. Enhancing chat language models by scaling high-quality instructional conversations. In *Proceedings of the 2023 Conference on Empirical Methods in Natural Language Processing*, pp. 3029–3051, 2023.

Dubey, A., Jauhri, A., Pandey, A., Kadian, A., Al-Dahle, A., Letman, A., Mathur, A., Schelten, A., Yang, A., Fan, A., et al. The llama 3 herd of models. *arXiv preprint arXiv:2407.21783*, 2024.

Engstrom, L. Dsdm: Model-aware dataset selection with datamodels. In *Forty-first International Conference on Machine Learning*, 2024.

Ge, C., Ma, Z., Chen, D., Li, Y., and Ding, B. Data mixing made efficient: A bivariate scaling law for language model pretraining. *arXiv preprint arXiv:2405.14908*, 2024.

Ge, Y., Hua, W., Mei, K., Tan, J., Xu, S., Li, Z., Zhang, Y., et al. Openagi: When llm meets domain experts. *Advances in Neural Information Processing Systems*, 36: 5539–5568, 2023.

Hendrycks, D., Burns, C., Kadavath, S., Arora, A., Basart, S., Tang, E., Song, D., and Steinhardt, J. Measuring mathematical problem solving with the math dataset. *NeurIPS*, 2021.

Hu, E. J., Shen, Y., Wallis, P., Allen-Zhu, Z., Li, Y., Wang, S., Wang, L., and Chen, W. Lora: Low-rank adaptation of large language models. *arXiv preprint arXiv:2106.09685*, 2021.

Joshi, M., Choi, E., Weld, D. S., and Zettlemoyer, L. Triviaqa: A large scale distantly supervised challenge dataset for reading comprehension. In *Proceedings of the 55th Annual Meeting of the Association for Computational Linguistics (Volume 1: Long Papers)*, pp. 1601–1611, 2017.

Kwiatkowski, T., Palomaki, J., Redfield, O., Collins, M., Parikh, A., Alberti, C., Epstein, D., Polosukhin, I., Devlin, J., Lee, K., et al. Natural questions: a benchmark for question answering research. *Transactions of the Association for Computational Linguistics*, 7:453–466, 2019.

Li, M., Zhang, Y., He, S., Li, Z., Zhao, H., Wang, J., Cheng, N., and Zhou, T. Superfiltering: Weak-to-strong data filtering for fast instruction-tuning. In *Proceedings of the 62nd Annual Meeting of the Association for Computational Linguistics (Volume 1: Long Papers)*, pp. 14255–14273, August 2024a. doi: 10.18653/v1/2024.acl-long.769.

Li, M., Zhang, Y., Li, Z., Chen, J., Chen, L., Cheng, N., Wang, J., Zhou, T., and Xiao, J. From quantity to quality: Boosting llm performance with self-guided data selection for instruction tuning. In *Proceedings of the 2024 Conference of the North American Chapter of the Association for Computational Linguistics: Human Language Technologies (Volume 1: Long Papers)*, pp. 7595–7628, 2024b.

Liu, A., Feng, B., Xue, B., Wang, B., Wu, B., Lu, C., Zhao, C., Deng, C., Zhang, C., Ruan, C., et al. Deepseek-v3 technical report. *arXiv preprint arXiv:2412.19437*, 2024a.

Liu, W., Zeng, W., He, K., Jiang, Y., and He, J. What makes good data for alignment? a comprehensive study of automatic data selection in instruction tuning. In *The Twelfth International Conference on Learning Representations*, 2024b.

Lu, K., Yuan, H., Yuan, Z., Lin, R., Lin, J., Tan, C., Zhou, C., and Zhou, J. # instag: Instruction tagging for analyzing supervised fine-tuning of large language models. In *The Twelfth International Conference on Learning Representations*, 2024.

Paszke, A., Gross, S., Massa, F., Lerer, A., Bradbury, J., Chanan, G., Killeen, T., Lin, Z., Gimelshein, N., Antiga, L., et al. Pytorch: An imperative style, high-performance deep learning library. *Advances in neural information processing systems*, 32, 2019.

Paul, M., Ganguli, S., and Dziugaite, G. K. Deep learning on a data diet: Finding important examples early in training. *Advances in neural information processing systems*, 34: 20596–20607, 2021.

Qin, Z., Chen, D., Zhang, W., Yao, L., Huang, Y., Ding, B., Li, Y., and Deng, S. The synergy between data and multi-modal large language models: A survey from co-development perspective, 2024. URL <https://arxiv.org/abs/2407.08583>.

Rafailov, R., Sharma, A., Mitchell, E., Manning, C. D., Ermon, S., and Finn, C. Direct preference optimization: Your language model is secretly a reward model. In *Thirty-seventh Conference on Neural Information Processing Systems*, 2023. URL <https://arxiv.org/abs/2305.18290>.

Raffel, C., Shazeer, N., Roberts, A., Lee, K., Narang, S., Matena, M., Zhou, Y., Li, W., and Liu, P. J. Exploring the limits of transfer learning with a unified text-to-text transformer. *Journal of machine learning research*, 21(140):1–67, 2020.

Song, F., Yu, B., Lang, H., Yu, H., Huang, F., Wang, H., and Li, Y. Scaling data diversity for fine-tuning language models in human alignment. In *Proceedings of the 2024 Joint International Conference on Computational Linguistics, Language Resources and Evaluation (LREC-COLING 2024)*, pp. 14358–14369, 2024.

Taori, R., Gulrajani, I., Zhang, T., Dubois, Y., Li, X., Guestrin, C., Liang, P., and Hashimoto, T. B. Stanford alpaca: An instruction-following llama model, 2023.

Tirumala, K., Simig, D., Aghajanyan, A., and Morcos, A. D4: Improving llm pretraining via document deduplication and diversification. *Advances in Neural Information Processing Systems*, 36:53983–53995, 2023.

Wang, Y., Ivison, H., Dasigi, P., Hessel, J., Khot, T., Chandu, K., Wadden, D., MacMillan, K., Smith, N. A., Beltagy, I., et al. How far can camels go? exploring the state of instruction tuning on open resources. *Advances in Neural Information Processing Systems*, 36:74764–74786, 2023.

Wei, J., Tay, Y., Bommasani, R., Raffel, C., Zoph, B., Borgeaud, S., Yogatama, D., Bosma, M., Zhou, D., Metzler, D., et al. Emergent abilities of large language models. *arXiv preprint arXiv:2206.07682*, 2022.

Wettig, A., Gupta, A., Malik, S., and Chen, D. Qurating: Selecting high-quality data for training language models. In *Forty-first International Conference on Machine Learning*, 2024.

Wolf, T., Debut, L., Sanh, V., Chaumond, J., Delangue, C., Moi, A., Cistac, P., Rault, T., Louf, R., Funtowicz, M., et al. Transformers: State-of-the-art natural language processing. In *Proceedings of the 2020 conference on empirical methods in natural language processing: system demonstrations*, pp. 38–45, 2020.

Xia, M., Malladi, S., Gururangan, S., Arora, S., and Chen, D. Less: Selecting influential data for targeted instruction tuning. In *Forty-first International Conference on Machine Learning*, 2024.

Yang, A., Yang, B., Zhang, B., Hui, B., Zheng, B., Yu, B., Li, C., Liu, D., Huang, F., Wei, H., et al. Qwen2. 5 technical report. *arXiv preprint arXiv:2412.15115*, 2024.

Ye, J., Liu, P., Sun, T., Zhou, Y., Zhan, J., and Qiu, X. Data mixing laws: Optimizing data mixtures by predicting language modeling performance. *arXiv preprint arXiv:2403.16952*, 2024.

Yu, Y., Khadivi, S., and Xu, J. Can data diversity enhance learning generalization? In *Proceedings of the 29th international conference on computational linguistics*, pp. 4933–4945, 2022.

Yue, X., Qu, X., Zhang, G., Fu, Y., Huang, W., Sun, H., Su, Y., and Chen, W. Mammoth: Building math generalist models through hybrid instruction tuning. In *The Twelfth International Conference on Learning Representations*, 2024.

Zellers, R., Holtzman, A., Bisk, Y., Farhadi, A., and Choi, Y. Hellaswag: Can a machine really finish your sentence? In *Proceedings of the 57th Annual Meeting of the Association for Computational Linguistics*, pp. 4791–4800, 2019.

Zhang, C., Zhong, H., Zhang, K., Chai, C., Wang, R., Zhuang, X., Bai, T., Qiu, J., Cao, L., Fan, J., et al. Harnessing diversity for important data selection in pretraining large language models. *arXiv preprint arXiv:2409.16986*, 2024.

Zhao, H., Du, L., Ju, Y., Wu, C., and Pan, T. Beyond iid: Optimizing instruction learning from the perspective of instruction interaction and dependency. *arXiv preprint arXiv:2409.07045*, 2024a.

Zhao, Y., Yu, B., Hui, B., Yu, H., Huang, F., Li, Y., and Zhang, N. L. A preliminary study of the intrinsic relationship between complexity and alignment. *arXiv preprint arXiv:2308.05696*, 2023.

Zhao, Y., Huang, J., Hu, J., Wang, X., Mao, Y., Zhang, D., Jiang, Z., Wu, Z., Ai, B., Wang, A., et al. Swift: a scalable lightweight infrastructure for fine-tuning. *arXiv preprint arXiv:2408.05517*, 2024b.

Zhou, C., Liu, P., Xu, P., Iyer, S., Sun, J., Mao, Y., Ma, X., Efrat, A., Yu, P., Yu, L., et al. Lima: Less is more for alignment. *Advances in Neural Information Processing Systems*, 36, 2024.

## Appendix

Our appendix is organized as follows:

- Sec. A: The **symbols** used in this paper.
- Sec. B: The **details** about **experiments and DAAR implementation**, including the construction of data pools (Sec. B.1), the benchmarks (Sec. B.2), the training & evaluation implementation (Sec. B.3), the implementation of baselines (Sec. B.4), the visualization of baseline’s selected data samples (Sec. B.5), the implementation of the synthetic data generation (Sec. B.6), the implementation of seed generation & clustering (Sec. B.7), and the prompts for the generation stage (Sec. B.8).
- Sec C: The **full proof** for theoretical results are presented in Section 4.
- Sec D: The **more experimental results**, including the visualization results of embeddings on Llama3.1-8B & Qwen2.5-7B (Sec D.1), the visualization results of inter- & intra-diversity distributions (Sec D.2), the similarity analysis in generated centroid quantities (Sec. D.3), the similarity analysis in generated centroid domains (Sec. D.4), the DAAR layer selection protocol (Sec. D.5), the comprehensive training dynamics (Sec. D.6), the validation of inter-diversity and intra-diversity (Sec. D.7) and the complete results of **DAAR** with baselines on all LLMs (Sec. D.8).

## A. Notation

For ease of reading and reference, we present all mathematical symbols used in this paper in Table 3.

Table 3. Symbol Notation

Symbol	Description	Symbol	Description
$\mathcal{D}$	Composite dataset	$\mathcal{D}_k$	Distinct domain dataset
$x_i^{(k)}$	Raw $i$ -th data sample in domain- $k$	$\mathbf{x}_i^{(k)}$	Embedded $i$ -th data sample in domain- $k$
$N_k$	Number of $\mathcal{D}_k$ data samples	$\mathcal{C}_k$	Domain centroid of $k$
$\phi_{\text{inter}}$	Sample-level cross-domain similarity	$\Phi_{\text{inter}}$	Global inter-diversity
$\phi_{\text{intra}}$	Sample similarity to its domain centroid	$\Phi_{\text{intra}}^{(k)}$	Domain-level variance of domain- $k$
$\mathcal{K}$	Set of labeled domains	$h_k$	Independent model of domain $k$
$l$	Loss function	$\mathcal{L}_{\mathcal{D}_k}$	Empirical risk
$\tilde{\mathcal{D}}_m$	Latent distribution of foundational capabilities	$\pi_{km}$	Mixture weights
$h_{\theta_m}$	Component model	$\theta_m^*$	Optimal predictor
$\mathcal{S}_k^{(0)}$	Generated centroids’ seed sample	$\mathcal{S}_k^{(t)}$	Generated centroid sample at $t$ -th round
$\mathcal{M}_{\text{ebd}}$	Embedding layer of LLM	$\mathcal{M}_3$	Layer-3 of LLM
$\mathcal{D}_{\text{probe}}$	DAAR training set	$\tau$	A similarity threshold
$\tilde{x}_i$	Data sample in $\mathcal{D}_{\text{probe}}$	$\tilde{y}_i$	Pseudo-label of $\tilde{x}_i$
$\psi_{\text{dom}}$	A MLP-based domain classifier	$\psi_{\text{div}}$	A MLP-based entropy predictor
$p_k(\tilde{x})$	Domain predicted probability by $\psi_{\text{dom}}$	$\hat{H}(\mathbf{x})$	Predictive entropy by $\psi_{\text{dom}}$
$\mathcal{L}_{\text{dom}}$	Cross-entropy loss of $\psi_{\text{dom}}$	$\mathcal{L}_{\text{div}}$	MSE loss of $\psi_{\text{dom}}$

## B. Experiments and Method Details

### B.1. Construction of Data Pool

To investigate data selection from large data pools and its impact on the mixture of downstream tasks, we construct a data pool with distinct properties to mimic practical settings. We select the following datasets to evaluate specific abilities:

- **Common Sense: Dolly-15K** (Conover et al., 2023) with 15,011 samples, an open source dataset of instruction-following records generated by thousands of Databricks employees in several of the behavioral categories.

- **Reasoning:** **Cot-en** (Chung et al., 2024) with 74,771 samples, is created by formatting and combining nine CoT datasets released by FLAN.
- **Mathematics:** **Math-Instruct** (Yue et al., 2024) with 262,039 samples, is compiled from 13 math rationale datasets, six of which are newly curated by this work. It uniquely ensures extensive coverage of diverse mathematical fields.
- **Coding:** **Code-Alpaca** (Chaudhary, 2023) with 20,016 samples, is constructed from real-world code examples, providing a rich set of tasks designed to guide models in generating accurate and functional code.

Each dataset was initially filtered and randomly reduced to 10,000 entries, resulting in a combined data pool of 40,000 entries. Specifically, for the Math-Instruct dataset, due to its inclusion of CoT and certain coding capabilities, we extract a highly mathematics-related subset and use regular expressions to filter out the coding-related content (including 'program', 'python', 'def', 'import', 'print', 'return'), ensuring it remains within the domain of mathematics.

## B.2. Benchmarks

To evaluate the models' true capabilities and performance across different domains, we follow the approach of major open-source LLMs (e.g., the Llama3 series (Dubey et al., 2024) and Qwen2 series (Yang et al., 2024)) and select the following widely used evaluation sets. All evaluations were conducted on the OpenCompass platform<sup>2</sup>.

- **Common Sense:** **NQ** (Kwiatkowski et al., 2019) and **TriviaQA** (Joshi et al., 2017), which cover factual knowledge-based questions of varying difficulty.
- **Reasoning:** **HellaSwag** (Zellers et al., 2019), which effectively evaluates the model's comprehensive reasoning ability.
- **Mathematics:** **GSM8K** (Cobbe et al., 2021) and **MATH** (Hendrycks et al., 2021) benchmarks, which encompass problems ranging from elementary to competition-level difficulty.
- **Coding:** **MBPP** (Austin et al., 2021) and **HumanEval** (Chen et al., 2021), which include evaluations of basic coding abilities in Python. We use the average of various metrics to demonstrate the models' overall performance across different domains.

Considering the numerous evaluation tasks, utilizing the complete evaluation set would result in significant time expenditure. To accelerate the evaluation process while maintaining fairness and accuracy, we randomly tailor the original evaluation sets into evaluation subsets, as detailed in Table 4. **All experiments were conducted using this consistent setup** to ensure the fairness of the experiments.

Table 4. Number of samples in various evaluation benchmarks' datasets.

Number of Samples	Common Sense		Reasoning		Mathematics		Coding	
	NQ	Triviaqa	Hellaswag	GSM8K	MATH	MBPP	HumanEval	
<b>Original</b>	3,610	8,837	10,042	1,319	5,000	974	164	
<b>Utilized</b>	3,610	5,000	10,042	500	1,000	500	164	

## B.3. Training and Evaluation Details

**Platform** We implement our approaches using PyTorch (Paszke et al., 2019) v2.4.1, coupled with PEFT v0.12.0 and the Transformers library (Wolf et al., 2020) v4.45.2. Experiments are conducted on a computing platform equipped with four NVIDIA A100 GPUs (40GB), with pre-trained LLMs loaded as 16-bit floating-point numbers. The specific data-model development processes are completed in Data-Juicer Sandbox (Chen et al., 2024c), via integration with the ms-swift (Zhao et al., 2024b) training repository, and the OpenCompass (Contributors, 2023) evaluation repository.

<sup>2</sup><https://opencompass.org.cn/>

**Training Details** In our experimental setup, we employ Low-Rank Adaptation (LoRA) (Hu et al., 2021) adapters for the fine-tuning process, utilizing a LoRA-rank of 8 and a LoRA-alpha of 16. The learning rate was consistently maintained at  $5 \times 10^{-5}$  across all experiments to ensure uniformity in training dynamics. We utilize a batch size of 4 and set the maximum sequence length to 2048 tokens to accommodate the model’s capacity. To optimize the training process, a warmup ratio of 0.05 was applied and a validation ratio of 0.03 was used. The training was conducted over a single epoch, balancing computational efficiency with the need for effective model adaptation. Following some effective instruction-tuning work (Zhou et al., 2024; Lu et al., 2024), we set the size of our subset to 8,000 entries, which constitutes 20% of the data pool.

**Evaluation Details** Following the guidelines provided by OpenCompass (Contributors, 2023), we adhered to the default settings for our evaluation process. We select the hf-type as *base* and utilized a batch size of *16* to ensure efficient processing. For most tasks, we employ the *gen* mode, while for the Hellaswag task, we opt for the *ppl* mode to better assess perplexity.

#### B.4. Implementation of Baselines

We select the following representative methods and works related to data selection as our baselines to evaluate their performance in the context of a mixture of downstream tasks.

**RANDOM SELECTION(RAND)** A random selection of 8,000 data samples from the data pool was made, which to some extent reflects the distribution characteristics of the original data pool.

**INSTRUCTION LENGTH (IL)** The length of the instruction can be considered a measure of input complexity. It is widely believed (Cao et al., 2023; Zhao et al., 2023) that more complex data is beneficial for enhancing model capabilities. Therefore, we select a subset of 8,000 entries with the maximum number of words (based on spaces) in the concatenation of Instruction and Input as part of the filtering process.

**ALPAGASUS (CHEN ET AL., 2024D)** Using prompts to directly score and annotate the quality of the data leverages the powerful cognitive abilities of LLMs for evaluation and selection. Based on the original work, we use the GPT-3.5-Turbo API to score the data with the following prompt:

##### Prompt 1: Implementation of ALPAGASUS

###### System Prompt:

We would like to request your feedback on the performance of AI assistant in response to the instruction and the given input displayed following.

Instruction: [Instruction]

Input: [Input]

Response: [Response]

###### User Prompt:

Please rate according to the accuracy of the response to the instruction and the input. Each assistant receives a score on a scale of 0 to 5, where a higher score indicates a higher level of accuracy. The generated scores can be precise to decimal points, not just in increments of 0.5. Please first output a single line containing the value indicating the scores. In the subsequent line, please provide a comprehensive explanation of your evaluation, avoiding any potential bias.

The distribution of direct ratings for the 40,000 data pool is shown in Fig. 3. Although the original paper’s prompts were strictly followed and efforts were made to minimize potential bias, most scores still clustered around 5. Since we require a uniform selection of 8,000 data samples, we randomly select the subset with a rating of 5 to serve as the baseline data.

**INSTAG (LU ET AL., 2024)** first utilizes ChatGPT to tag the samples based on semantics and intentions, then trains a LLaMA-based tagger on the ChatGPT tags to tag data. They use the number of tags as a proxy for complexity. We directly use ChatGPT-3.5-Turbo as a tagger to achieve better performance. Following the original paper, the prompt is as follows.

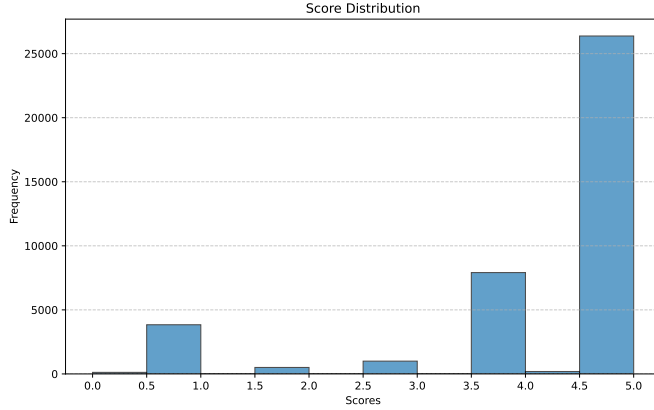


Figure 3. The distribution of the score by ALPAGASUS.

## Prompt 2: Implementation of INSTAG COMPLEXITY

### System Prompt:

You are a tagging system that provides useful tags for instruction intentions to distinguish instructions for a helpful AI assistant. Below is an instruction:

```
[begin]
{Instruction + Input}
[end]
```

### User Prompt:

Please provide coarse-grained tags, such as "Spelling and Grammar Check" and "Cosplay", to identify main intentions of above instruction. Your answer should be a list including titles of tags and a brief explanation of each tag. Your response have to strictly follow this JSON format: [ "tag": str, "explanation": str]. Please response in English.

A total of 19,585 tags were assigned across 40,000 data samples, with the distribution shown below. Subsequently, based on the procedures outlined in the original text, tags were deduplicated as follows: 1) filter out long-tail tags that appear fewer than  $\alpha$  times in the entire annotated dataset, and 2) transform all tags to lowercase to mitigate the influence of capitalization.

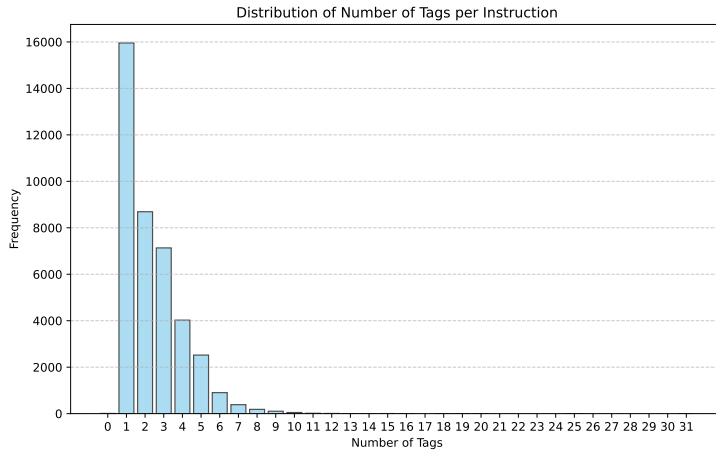


Figure 4. The distribution of the tags by INSTAG.

- **INSTAG COMPLEXITY (INSTAG-C):** To reduce redundancy, we apply a threshold of  $\alpha = 5$ , resulting in a set of 1,948 valid tags. Following the definition of Complexity, we select the top 8,000 entries with the highest tag counts. Specifically, there are 8,211 entries with more than three tags, so we include all records with more than four tags and randomly supplement from those with exactly four tags until reaching a total of 8,000 entries.
- **INSTAG DIVERSITY (INSTAG-D):** For Diversity, we use  $\alpha = 1$  to reduce redundancy. The algorithm employed involves sorting all data in descending order based on the number of tags, and prioritizing records with more tags. To ensure dataset diversity, a tag is only added to the final dataset if it increases the overall size of the tag set. This approach captures a broader range of unique tags, thereby enhancing the diversity and representativeness of the dataset.

**SUPERFILTER (LI ET AL., 2024A)** introduces a method that astonishingly utilizes a small GPT2 model to successfully filter out the high-quality subset from the existing GPT4-generated instruction tuning dataset. The core concept is the instruction-following difficulty (IFD) score. By meticulously following this methodology, we utilize GPT-2 to select 8,000 data samples.

**DEITA (LIU ET AL., 2024B)** is an open-sourced project designed to facilitate Automatic Data Selection for instruction tuning in LLMs. It delves into the relationships between data complexity, quality, and diversity, and develops a series of methodologies. Specifically, we utilize it as the following three baselines:

- **DEITA COMPLEXITY (DEITA-C):** Enhances instruction complexity by evolving examples with techniques like adding constraints. ChatGPT ranks these evolved samples for complexity, and the scores train a LLaMA-1-7B model to predict complexity in new instructions, refining complexity assessment. We utilize its LLaMA-1-7B-based complexity-scorer to evaluate the data pool and select the top 20% of them to reach 8,000 entries.
- **DEITA QUALITY (DEITA-Q):** Enhances response quality by prompting ChatGPT to iteratively improve helpfulness, relevance, depth, creativity, and detail. After five iterations, ChatGPT ranks and scores the responses, providing nuanced quality distinctions. These scores train an LLaMA-1 7B model to predict quality scores for new instruction-response pairs. We utilize its LLaMA-1-7B-based quality scorer to evaluate the data pool and select the top 20% of them to reach 8,000 entries.
- **DEITA DITA (DEITA-D):** Data-Efficient Instruction Tuning for Alignment, it selects data by combining complexity and quality into an evol score, prioritizing higher scores. It uses the REPR FILTER to iteratively add samples, ensuring diversity and avoiding redundancy, resulting in a balanced dataset of complexity, quality, and diversity. Following its methodology, we gain 8,000 entries as a baseline.

## B.5. Visualization of Baseline’s Selected Data

We project all baseline-selected data samples through Llama3.1-8B’s, Qwen2-7B’s and Qwen2.5-7B’s embedding layer and visualize their distributions via t-SNE dimensionality reduction in Fig. 5, Fig. 6 and Fig. 7 respectively. This visualization provides intuitive insights into how different data selection strategies handle domain-mixed data. Three key observations emerge:

- 1 Certain methods (notably INSTRUCTION LENGTH, DEITA-C, and DEITA-Q baselines) exhibit significant distributional bias against coding-domain samples, correlating with their poor HumanEval performance in Table 10.
- 2 The visualization reveals inherent challenges in maintaining original data distributions when handling domain-undetermined samples.
- 3 Despite observable distribution shifts, not all methods show proportional performance degradation, aligning with our theoretical analysis in Section 4 about the link between latent distribution and LLM’s fundamental capabilities.

## B.6. Implementation of the Synthetic Data Generation

For the generation of synthetic data, we utilize the `model.generate` function from the PyTorch library. Key parameters included setting `max-new-tokens` to `2048` to control the length of the output, enabling `do-sample` to `True` to allow sampling, and configuring `top-p` to `0.95` and `temperature` to `0.9` to ensure diversity in the generated content. During the content extraction phase, we employ `regular expressions` to efficiently extract and structure the desired information.

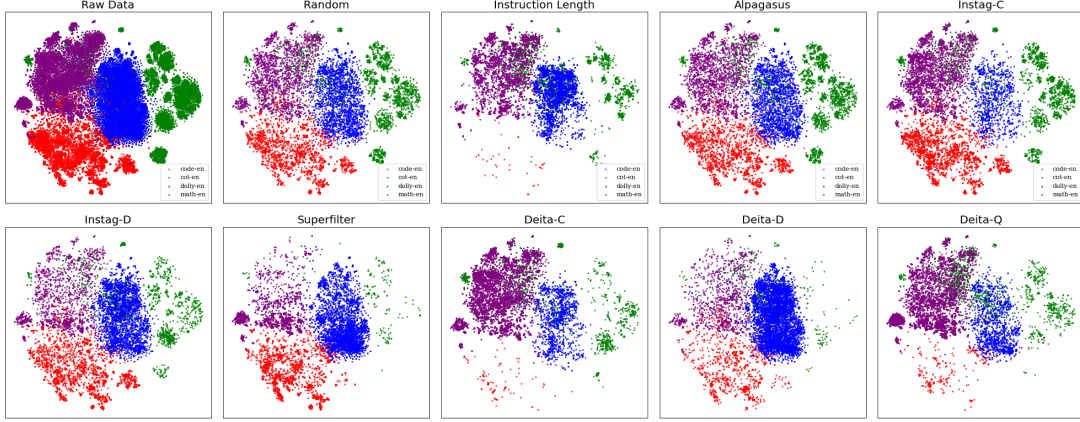


Figure 5. t-SNE visualization of data samples selected by different baselines using Llama3.1-8B embeddings. While original labels were removed during training, we preserve them in the legend for interpretability.

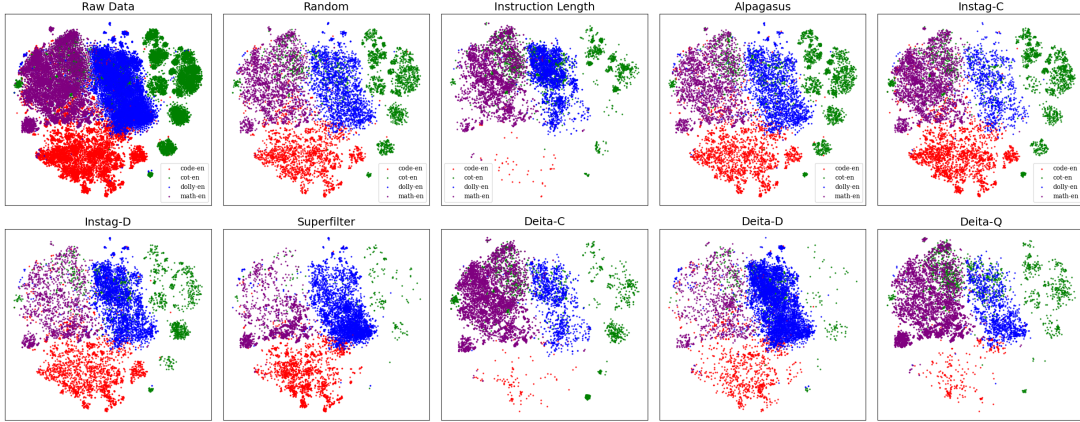


Figure 6. t-SNE visualization of data samples selected by different baselines using Qwen2-7B embeddings. While original labels were removed during training, we preserve them in the legend for interpretability.

## B.7. Implementation of Seed Generation & Clustering

Due to the difficulty of pre-trained LLMs in providing accurate and coherent responses, we utilize their corresponding Instruct versions for centroid data generation. Specifically, we apply Llama3.1-8B-Instruct for Llama3.1-8B, Qwen2-7B-Instruct for Qwen2-7B, and Qwen2.5-7B-Instruct for Qwen2.5-7B. The domain description and the zero-shot prompt used in the Seed Generation phase are as follows. When clustering reward training data based on the seed, we select 5,000 entries that match the distribution of the fine-tuning data but do not overlap with it. This practice has proven that even a small amount of data can effectively train a reward probe module of **DAAR**.

### Prompt 3: Domain's Description

**Common Sense:** Common sense generally includes a knowledge-based question and its corresponding answer, without reasoning.

**Reasoning:** Reasoning involves the ability to think logically about a situation or problem, to draw conclusions from available information, and to apply knowledge in new situations.

**Mathematics:** Mathematical skills include the ability to perform calculations, understand mathematical concepts, solve hard and professional math problems, and apply mathematical reasoning.

**Coding:** Design and generate specific code programs, or apply algorithms and data structures, with code generation in the Output.

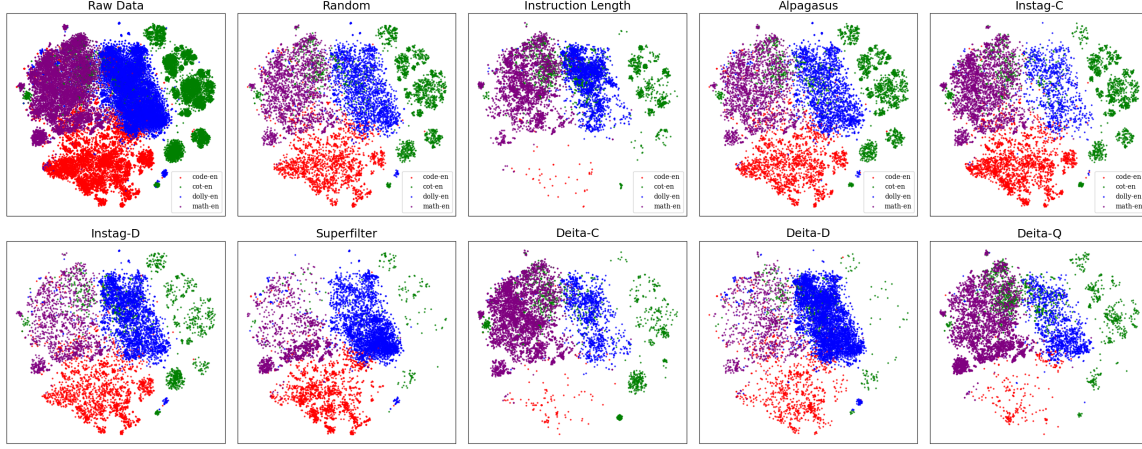


Figure 7. t-SNE visualization of data samples selected by different baselines using Qwen2.5-7B embeddings. While original labels were removed during training, we preserve them in the legend for interpretability.

#### Prompt 4: Seed Generation Zero-shot Prompt

You are an AI model with expertise in {selected\_domain}. Here's a brief description of this domain: {Prompt 1}

Generate 5 different instruction pairs related to this field with various lengths. Maintain the index format: Instruction [1 ... 5].

The response should include three parts:

1. Instruction: A clear command or question that can be understood by the assistant.
2. Input: Any information provided to help it understand the instruction. If there is no need to generate, just keep it empty.
3. Output: The expected answer or action.

Keep the generated content focused on {selected\_domain}. And do not involve {unselected\_domains} related knowledge.

#### B.8. Prompts for the Generation Stage

##### Prompt 5: Instruction Pairs Generation

You are an AI model with expertise in {selected\_domain}. Here's a brief description of this domain: {Prompt 1}

Generate only an instruction pair related to this field. The response should include three parts:

Instruction: A clear command or question that can be understood by the assistant.

Input: Any information provided to help it understand the instruction. If there is no need to generate, just keep empty.

Output: The expected answer or action.

Keep the generated content focused on {selected\_domain}. Do not involve {unselected\_domain} related knowledge.

Note that you should generate content strongly unrelated and different to these examples to ensure diversity in the generated output:

Counterexample: {}

The format of the generated content should be: Instruction: [], Input: [], Output: [].

## C. Proof of Section 4

### C.1. Proof of Proposition 4.3

**Lemma C.1** (Cross-Domain Risk Decomposition). *Under Assumption 4.1, the average cross-domain risk becomes:*

$$\mathbb{E}_{k \sim \mathcal{K}} \mathcal{L}_{\mathcal{D}_k} \left( \sum_{m=1}^M \pi_{km} h_{\theta_m} \right) = \sum_{m=1}^M \lambda_m \mathbb{E}_{\tilde{\mathcal{D}}_m} \left[ l \left( \sum_{m'=1}^M \pi_{km'} h_{\theta_{m'}}(x), y \right) \right], \quad (21)$$

where  $\lambda_m = \mathbb{E}_k[\pi_{km}]$  represents global activation of capability  $m$ .

*Proof.* Under the finite variance condition  $\mathbb{E}_{\tilde{\mathcal{D}}_m} [\|l\|_2^2] < \infty$ , Fubini's theorem holds, and results in:

$$\begin{aligned} \mathbb{E}_k \mathcal{L}_{\mathcal{D}_k} &= \mathbb{E}_k \mathbb{E}_{(x,y) \sim \mathcal{D}_k} [l(\sum_m \pi_{km} h_{\theta_m}(x), y)] \\ &= \mathbb{E}_k \mathbb{E}_{m \sim \pi_k} \mathbb{E}_{\tilde{\mathcal{D}}_m} [l(\sum_{m'} \pi_{km'} h_{\theta_{m'}}(x), y)] \\ &= \sum_{m=1}^M \lambda_m \mathbb{E}_{\tilde{\mathcal{D}}_m} [l(\sum_{m'} \pi_{km'} h_{\theta_{m'}}(x), y)] \end{aligned} \quad (22)$$

□

**Theorem C.2** (Global Optimality Condition). *Under Assumptions 4.1-4.2, the optimal predictors  $\{h_{\theta_m^*}\}$  minimize the cross-domain risk when:*

$$\forall m, \theta_m^* = \operatorname{argmin}_{\theta} \mathbb{E}_{\tilde{\mathcal{D}}_m} [l(h_{\theta}(x), y)]. \quad (23)$$

*Proof.* Taking derivatives of Lemma C.1's right-hand side:

$$\frac{\partial}{\partial \theta_m} \sum_{m'=1}^M \lambda_{m'} \mathbb{E}_{\tilde{\mathcal{D}}_{m'}} [\cdot] = \lambda_m \mathbb{E}_{\tilde{\mathcal{D}}_m} \left[ \frac{\partial l}{\partial h} \frac{\partial h_{\theta_m}}{\partial \theta_m} \right] + \sum_{m' \neq m} \lambda_{m'} \mathbb{E}_{\tilde{\mathcal{D}}_{m'}} \left[ \frac{\partial l}{\partial h} \frac{\partial h_{\theta_m}}{\partial \theta_m} \right].$$

By strong convexity and optimality of  $\theta_m^*$ , all terms vanish when  $\theta_m = \theta_m^*$ . □

### C.2. Proof of Proposition 4.4

**Proof of Inter-Diversity** To prove the inter-diversity decomposition as given in Proposition 4.4, we begin by considering the inter-diversity metric  $\Phi_{\text{inter}}$ , defined as the expected pairwise distance between domain centroids from Eq (3):

$$\Phi_{\text{inter}} = \mathbb{E}_{k \neq l} [\|\mathcal{C}_k - \mathcal{C}_l\|_2]. \quad (24)$$

Substituting the expression for each domain centroid (Eq (10))  $\mathcal{C}_k = \sum_{m=1}^M \pi_{km} \mathcal{C}_m$ , we have:

$$\|\mathcal{C}_k - \mathcal{C}_l\|_2 = \left\| \sum_{m=1}^M \pi_{km} \mathcal{C}_m - \sum_{n=1}^M \pi_{ln} \mathcal{C}_n \right\|_2. \quad (25)$$

Applying the triangle inequality and expanding, the distance becomes:

$$= \left\| \sum_{m=1}^M \sum_{n=1}^M (\pi_{km} - \pi_{ln}) \mathcal{C}_m + \pi_{ln} \mathcal{C}_n \right\|_2. \quad (26)$$

Taking the expectation over all domain pairs  $k \neq l$  and using linearity, we have:

$$\Phi_{\text{inter}} = \mathbb{E}_{k \neq l} \left[ \sum_{m=1}^M \sum_{n=1}^M (\pi_{km} \pi_{ln}) \|\mathcal{C}_m - \mathcal{C}_n\|_2 \right]. \quad (27)$$

Recognizing that  $\lambda_m = \mathbb{E}_k[\pi_{km}]$  is the expected activation of capability  $m$ , we can simplify further:

$$= \sum_{m=1}^M \sum_{n=1}^M \lambda_m \lambda_n \|\mathcal{C}_m - \mathcal{C}_n\|_2. \quad (28)$$

This completes the proof, showing that the inter-diversity metric is determined by the expected pairwise distances between latent capability centroids, weighted by their activation probabilities.

**Proof of Intra-Diversity** The intra-diversity metric for domain  $k$ , denoted as  $\Phi_{\text{intra}}^{(k)}$ , measures the variance of data samples within the domain relative to its centroid  $\mathcal{C}_k$ . We aim to show that:

$$\Phi_{\text{intra}}^{(k)} \leq \sum_{m=1}^M \pi_{km} \|\mathcal{C}_m - \mathcal{C}_k\|_2^2 + \mathbb{E}_{m \sim \pi_k} [\text{Var}(\tilde{\mathcal{D}}_m)]. \quad (29)$$

*Proof.* To prove this bound, we start by expressing the intra-diversity metric  $\Phi_{\text{intra}}^{(k)}$  as the expected squared distance from each sample  $\mathbf{x}_i^{(k)}$  to the domain centroid  $\mathcal{C}_k$  from Eq (5):

$$\Phi_{\text{intra}}^{(k)} = \frac{1}{N_k} \sum_{i=1}^{N_k} \|\mathbf{x}_i^{(k)} - \mathcal{C}_k\|_2^2. \quad (30)$$

Using the definition of the domain centroid (Eq (10))  $\mathcal{C}_k = \sum_{m=1}^M \pi_{km} \mathcal{C}_m$  in , we can decompose the squared distance for each sample:

$$\|\mathbf{x}_i^{(k)} - \mathcal{C}_k\|_2^2 = \|\mathbf{x}_i^{(k)} - \sum_{m=1}^M \pi_{km} \mathcal{C}_m\|_2^2. \quad (31)$$

Applying the variance decomposition, we have:

$$\|\mathbf{x}_i^{(k)} - \mathcal{C}_k\|_2^2 = \|\mathbf{x}_i^{(k)} - \sum_{m=1}^M \pi_{km} \mathcal{C}_m\|_2^2 = \sum_{m=1}^M \pi_{km} \|\mathbf{x}_i^{(k)} - \mathcal{C}_m\|_2^2 + \sum_{m=1}^M \pi_{km} \|\mathcal{C}_m - \mathcal{C}_k\|_2^2, \quad (32)$$

where the first term represents the variance within each latent capability, and the second term accounts for the distance between latent capability centroids and the domain centroid.

By taking the expectation over the samples in domain  $k$ , we get:

$$\Phi_{\text{intra}}^{(k)} \leq \sum_{m=1}^M \pi_{km} \|\mathcal{C}_m - \mathcal{C}_k\|_2^2 + \mathbb{E}_{m \sim \pi_k} [\text{Var}(\tilde{\mathcal{D}}_m)], \quad (33)$$

where  $\text{Var}(\tilde{\mathcal{D}}_m)$  represents the variance within the  $m$ -th latent capability. This completes the proof of the intra-diversity bound.  $\square$

## D. More Experimental Results

### D.1. Visualization of Embeddings on Llama3.1-8B & Qwen2.5-7B

We process concatenated data samples with “instruction”+“input”+“output” pairs through each LLM’s embedding layer, computing **mean token** embeddings for visualization. Beyond Qwen2-7B results in Fig. 1, we present the t-SNE visualization of data samples from Llama3.1-8 and Qwen2.5-7B with different distributions in Fig. 8 and Fig. 9. It is evident that, despite differences in architecture or model, the method of filtering data through Inter-Diversity and Intra-Diversity is effective. Notably, although the embedding distributions of different models are not identical, they exhibit similar behavior, indicating that the representations learned by the embedding layers are comparable.

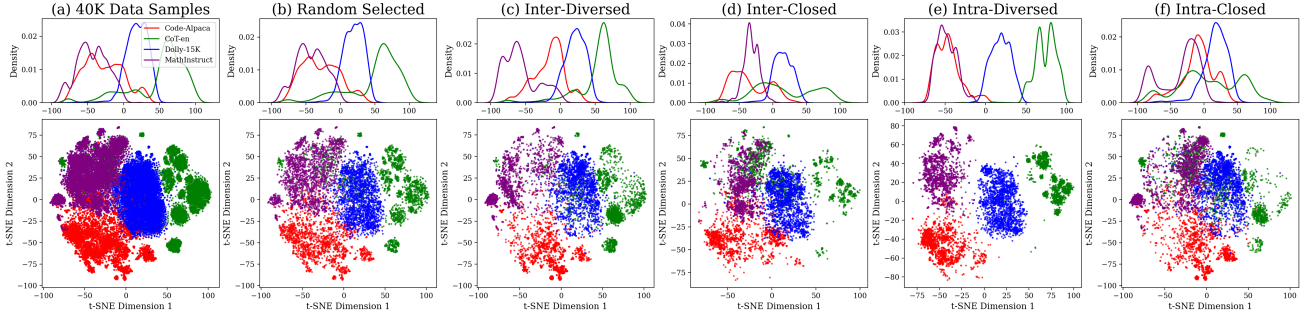


Figure 8. The t-SNE visualization of embeddings for data samples with different distributions on Llama3.1-8B. (a) The data pool of all 40,000 samples, (b) Randomly selected subset, (c) Distribution of data farthest from other domain centroids based on Inter-Diversity, (d) Distribution of data closest to other domain centroids based on Inter-Diversity, (e) Distribution of data closest to its own domain centroid based on Inter-Diversity, (f) Distribution of data farthest from its own domain centroid based on Inter-Diversity.

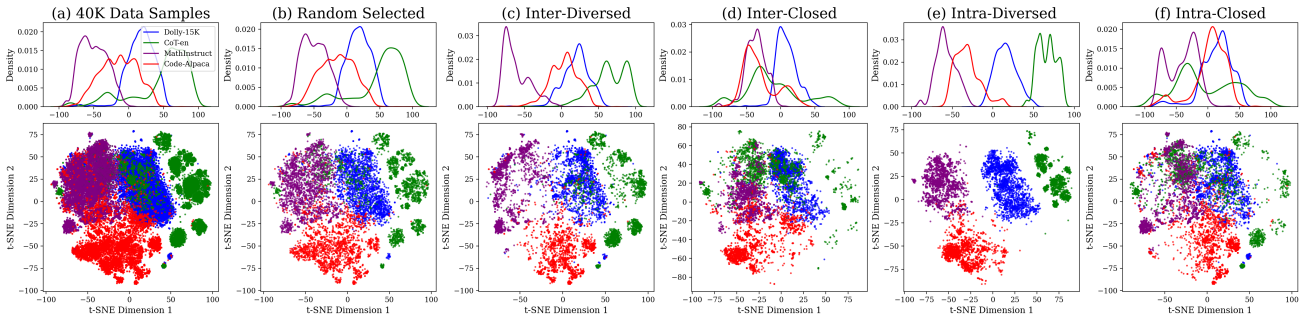


Figure 9. The t-SNE visualization of embeddings for data samples with different distributions on Qwen2.5-7B. (a) The data pool of all 40,000 samples, (b) Randomly selected subset, (c) Distribution of data farthest from other domain centroids based on Inter-Diversity, (d) Distribution of data closest to other domain centroids based on Inter-Diversity, (e) Distribution of data closest to its own domain centroid based on Inter-Diversity, (f) Distribution of data farthest from its own domain centroid based on Inter-Diversity.

## D.2. The Visualization of Inter- & Intra-Diversity Distribution Data

Using the Qwen2-7B model as an example, we construct data based on the Inter-Diversity and Intra-Diversity distribution methods, selecting a batch of data every 20%. The visualization process is shown in Fig. 10 and Fig. 11. As seen in the figures, the data gradually transitions from domain-aware diverse to domain-aware closed, indicating that our data construction method effectively controls the distribution of different data. However, it is important to note that t-SNE dimensionality reduction is used only for visualization purposes; during the reduction process, positional information is lost, and it cannot fully capture the true high-dimensional relationships between the data.

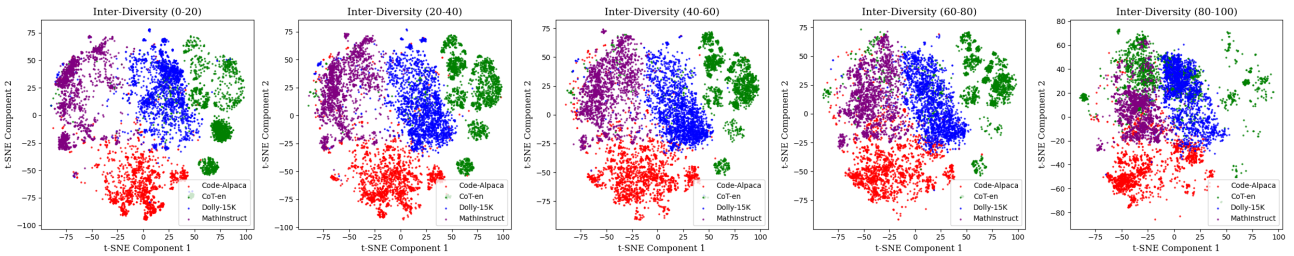


Figure 10. Data visualization (t-SNE) based on different Inter-Diversity distributions on Qwen2-7B.

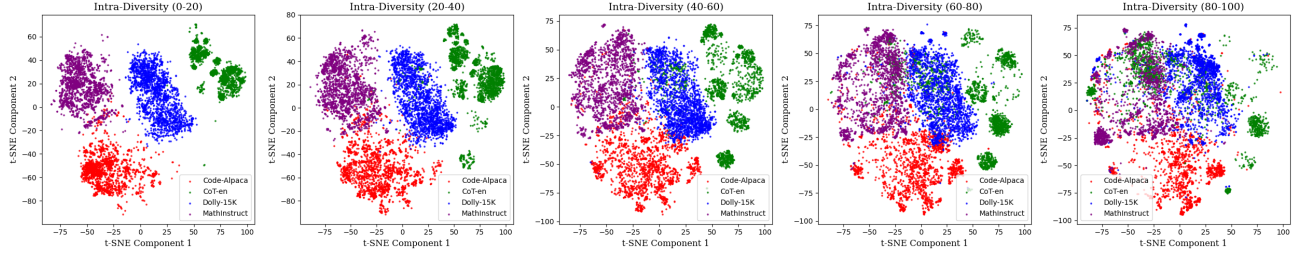


Figure 11. Data visualization (t-SNE) based on different **Intra-Diversity** distributions on Qwen2-7B.

### D.3. Similarity in Generated Centroid Quantities

To assess the impact of the amount of generated data on the accuracy of Domain Semantic Centroids, we select quantities of 10 and 30 samples for generation. Subsequently, we calculate the semantic cosine similarity between these two sets, with results presented in Table 5 (using Qwen2-7B and Llama3.1-8B as examples). The observed differences between varying data quantities were not significant, indicating that the generalization of the generated data is sufficient and further increasing the data quantity does not significantly enhance the accuracy of the centroids.

Table 5. Semantic cosine similarity between generated samples of size 10 and 30 across different domains.

Similarity of 10 & 30	Common Sense	Reasoning	Mathematics	Coding
<b>Qwen2-7B</b>	0.9686	0.9866	0.9919	0.9881
<b>Llama3.1-8B</b>	0.9851	0.9795	0.9685	0.9895

### D.4. Similarity in Generated Centroid Domains

To investigate whether there is a distinct separation between different domains generated, we compute the cosine similarity of semantic centroids across different domains. The experimental results are shown in Fig 12. It is evident that, compared to variations within the same domain at different data quantities, there are significant differences between different domains. This validates that this method of generating synthetic data can produce domain-representative data with clear distinction.

Notably, despite variations in model architecture and parameter count, the generated content consistently exhibits the greatest divergence between common sense, reasoning, and coding domains. Specifically, the discrepancy between common sense and coding, as well as reasoning and coding, is markedly pronounced. Conversely, the semantic difference between common sense and reasoning is relatively smaller. This pattern suggests that the models, although differing in complexity and size, exhibit varying sensitivity to different data types, highlighting their nuanced capability to distinguish between certain domain-specific characteristics while maintaining subtle distinctions in others.

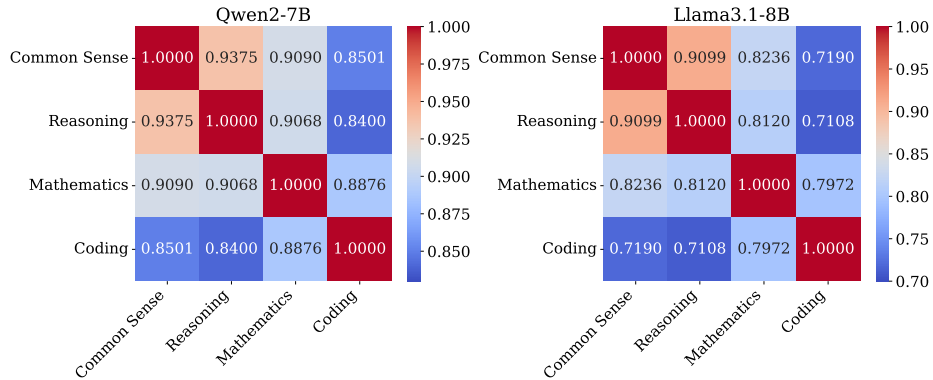


Figure 12. Semantic cosine similarity across different domains for generated samples of size 10.

### D.5. DAAR Layer Selection Protocol

To determine an appropriate layer for embedding **DAAR** into a large language model (LLM) that balances performance and computational cost, we first evaluate the capacity of different layers for domain awareness. Using Qwen2-7B as an example, we conduct t-SNE visualizations of Layer-5, Layer-10, Layer-15, Layer-20, Layer-25, and the last hidden layer, based on the average token vectors, as shown in Fig. 13.

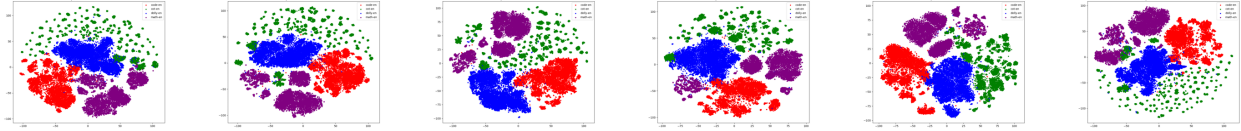


Figure 13. t-SNE visualization of mean token embeddings across Layer-5, Layer-10, Layer-15, Layer-20, Layer-25, and the last hidden layer of Qwen2-7B.

Our observations indicate that even at the early Layer-5, the model begins to exhibit classification capabilities across different datasets. This prompted us to focus on the initial five layers to enhance learning outcomes. Considering that data clustering is inherently influenced by the embedding layer, a natural approach was to directly connect to the embedding layer for training. However, the training results showed persistently high training loss and a validation accuracy of only about 0.6, indicating suboptimal learning performance. Furthermore, related studies indicate that LLMs can learn semantic understanding and perception in the early layers (Wei et al., 2022), consequently, we select Layer-3 for **DAAR**.

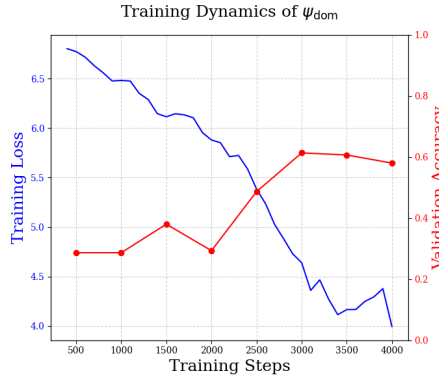


Figure 14. Training loss and validation process of Embedding Layer on Qwen2-7B.

### D.6. Comprehensive Training Dynamics

We present the training loss and validation results for two distinct models, Llama3.1-8B and Qwen2.5-7B, in Fig 15. It can be observed that across different models, the training process of **DAAR** method consistently ensures gradual convergence, achieving high domain predictability and calibrated entropy fitting.

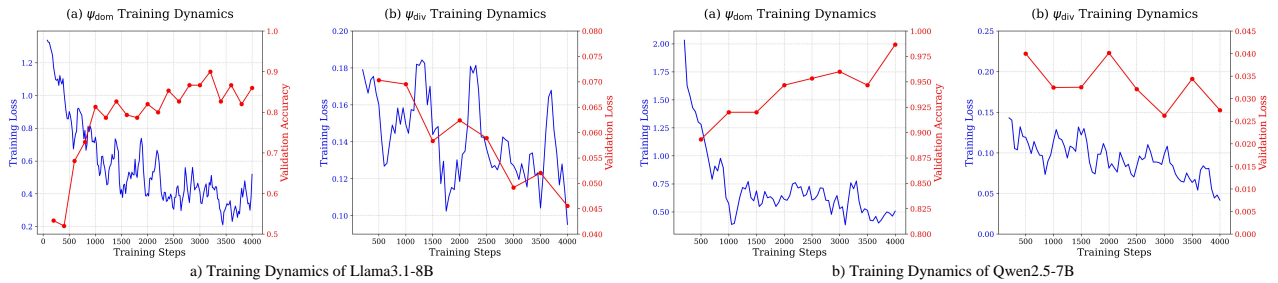


Figure 15. Training loss and validation process of the two training stages of **DAAR** on Llama3.1-8B and Qwen2.5-7B, showing the model gradually converging.

### D.7. Complete Validation Results of Inter-Diversity and Intra-Diversity

We present the complete experimental results of Llama3.1-8B, Qwen2-7B, and Qwen2.5-7B in the validation experiments in Tables 6, Tables 7, and Tables 8, respectively. It can be observed that for any complete dataset, the conclusions from Section 3.3 remain valid, specifically that the peak distribution of results is uneven, with significant differences among them.

Table 6. Validation Results of Inter-Diversity and Intra-Diversity on Llama3.1-8B across various benchmarks.

Llama3.1-8B	Common Sense		Reasoning	Mathematics		Coding		Avg
	NQ	TriviaQA	Hellaswag	GSM8K	MATH	MBPP	HumanEval	
<b>RAW</b>	14.13	65.90	74.62	54.80	7.90	5.00	28.66	35.86
<b>RAND</b>	21.99	64.83	74.72	55.70	14.50	5.10	24.09	37.27
Inter-Diversity (0-20)	19.28	65.79	74.44	54.90	6.50	4.30	35.06	37.18
Inter-Diversity (20-40)	21.91	65.48	74.54	52.50	16.65	5.70	26.53	37.62
Inter-Diversity (40-60)	23.70	65.14	74.86	56.40	17.15	5.00	24.40	38.09
Inter-Diversity (60-80)	22.42	64.52	74.76	55.10	14.60	7.40	31.10	38.56
<b>Inter-Diversity (80-100)</b>	<b>23.76</b>	<b>64.43</b>	<b>75.20</b>	<b>56.40</b>	<b>15.05</b>	<b>4.50</b>	<b>33.54</b>	<b>38.98</b>
Intra-Diversity (0-20)	22.08	65.08	75.00	54.70	16.20	4.40	33.54	38.71
Intra-Diversity (20-40)	22.41	64.44	74.66	52.60	15.30	4.20	27.44	37.29
Intra-Diversity (40-60)	22.12	64.74	74.87	54.00	16.00	6.00	27.44	37.88
Intra-Diversity (60-80)	20.83	64.30	74.36	52.20	14.90	4.50	35.98	38.15
<b>Intra-Diversity (80-100)</b>	<b>19.78</b>	<b>64.77</b>	<b>74.51</b>	<b>56.50</b>	<b>13.00</b>	<b>5.20</b>	<b>37.50</b>	<b>38.75</b>

Table 7. Validation Results of Inter-Diversity and Intra-Diversity on Qwen2-7B across various benchmarks.

Qwen2-7B	Common Sense		Reasoning	Mathematics		Coding		Avg
	NQ	TriviaQA	Hellaswag	GSM8K	MATH	MBPP	HumanEval	
<b>RAW</b>	8.03	59.58	73.00	78.00	5.70	5.00	60.98	41.47
<b>RAND</b>	13.28	58.27	73.00	75.35	35.36	52.20	63.72	<u>53.02</u>
<b>Inter-Diversity (0-20)</b>	<b>15.18</b>	<b>59.28</b>	<b>73.34</b>	<b>74.50</b>	<b>34.94</b>	<b>53.10</b>	<b>68.60</b>	<b>54.13</b>
Inter-Diversity (20-40)	13.77	58.42	73.18	73.60	32.55	53.00	64.33	52.69
Inter-Diversity (40-60)	14.62	58.58	73.35	72.50	34.50	52.50	61.28	52.47
Inter-Diversity (60-80)	14.31	58.60	73.33	74.80	33.90	51.40	60.68	52.43
Inter-Diversity (80-100)	9.30	57.72	73.14	74.60	28.00	51.30	63.42	51.07
Intra-Diversity (0-20)	12.64	58.54	73.35	75.10	8.75	51.10	61.59	48.72
Intra-Diversity (20-40)	14.17	58.78	73.10	74.10	29.20	52.10	63.41	52.12
Intra-Diversity (40-60)	15.24	58.57	73.12	74.70	32.50	51.80	64.02	52.85
Intra-Diversity (60-80)	14.02	57.40	73.06	75.20	32.20	53.50	66.77	53.16
<b>Intra-Diversity (80-100)</b>	<b>11.91</b>	<b>57.88</b>	<b>73.29</b>	<b>75.00</b>	<b>36.05</b>	<b>52.50</b>	<b>66.16</b>	<b>53.25</b>

Table 8. Validation Results of Inter-Diversity and Intra-Diversity on Qwen2.5-7B across various benchmarks.

Qwen2.5-7B	Common Sense		Reasoning	Mathematics		Coding		Avg
	NQ	TriviaQA	Hellaswag	GSM8K	MATH	MBPP	HumanEval	
<b>RAW</b>	8.84	58.14	72.75	78.20	9.10	7.40	78.05	44.64
<b>RAND</b>	11.46	57.85	73.08	78.90	13.15	62.50	71.65	<u>52.65</u>
Inter-Diversity (0-20)	13.23	58.15	73.27	78.70	11.45	62.30	69.21	52.33
Inter-Diversity (20-40)	10.81	58.11	73.02	77.90	16.95	62.30	68.29	52.48
<b>Inter-Diversity (40-60)</b>	10.75	57.89	72.90	73.30	26.70	62.80	69.51	<b><u>53.41</u></b>
Inter-Diversity (60-80)	10.43	58.19	73.10	78.40	17.05	62.80	71.95	53.13
Inter-Diversity (80-100)	10.00	58.10	73.11	77.30	16.45	62.30	67.07	52.05
<b>Intra-Diversity (0-20)</b>	10.68	58.52	73.18	80.10	25.80	62.50	68.90	<b><u>54.24</u></b>
Intra-Diversity (20-40)	11.21	58.14	73.02	79.50	17.75	62.90	67.38	52.84
Intra-Diversity (40-60)	11.57	58.11	72.94	76.00	15.65	62.50	65.25	51.72
Intra-Diversity (60-80)	10.89	57.91	72.92	75.80	11.35	62.00	66.16	51.00
Intra-Diversity (80-100)	12.79	58.09	73.21	75.40	16.05	62.50	49.39	49.63

## D.8. Complete Results of DAAR with Baselines

Additionally, we include the complete results of **DAAR** and the comparative baselines in the three tables: Table 9, Table 10 and Table 11. The results illustrate the challenges of the scenario, particularly for the Qwen2 series, where baseline methods struggle to outperform random selection. Furthermore, they demonstrate the robustness and effectiveness of our approach, consistently achieving the highest average scores across different models.

 Table 9. Performance of **DAAR** with baselines on Llama3.1-8B across various benchmarks.

Llama3.1-8B	Common Sense		Reasoning	Mathematics		Coding		Avg
	NQ	TriviaQA	Hellaswag	GSM8K	MATH	MBPP	HumanEval	
<b>RAW</b>	14.13	65.90	74.62	54.80	7.90	5.00	28.66	35.86
<b>RAND</b>	21.99	64.83	74.72	55.70	14.50	5.10	24.09	37.27
<b>INSTRUCTION LEN</b>	15.34	63.60	73.73	54.00	15.40	3.60	30.80	36.64
<b>ALPAGASUS (Chen et al., 2024d)</b>	21.57	64.37	74.87	55.20	17.65	4.60	16.16	36.34
<b>INSTAG-C (Lu et al., 2024)</b>	18.12	64.96	74.01	55.70	15.50	4.80	37.81	38.70
<b>INSTAG-D (Lu et al., 2024)</b>	21.94	64.69	74.87	54.80	12.80	4.10	9.76	34.71
<b>SUPERFILTER (Li et al., 2024a)</b>	22.95	64.99	76.39	57.60	6.05	2.60	40.55	<u>38.73</u>
<b>DEITA-C (Liu et al., 2024b)</b>	15.58	64.97	74.21	55.00	13.05	4.60	34.46	37.41
<b>DEITA-Q (Liu et al., 2024b)</b>	19.57	64.22	75.15	54.00	7.20	4.20	28.35	36.10
<b>DEITA-D (Liu et al., 2024b)</b>	20.97	63.32	75.10	54.90	7.00	4.00	31.71	36.71
<b>DAAR (Ours)</b>	20.08	64.55	74.88	54.8	15.30	4.70	37.50	<b><u>38.83</u></b>

Table 10. Performance of DAAR with baselines on Qwen2-7B across various benchmarks.

Qwen2-7B	Common Sense		Reasoning	Mathematics		Coding		Avg
	NQ	TriviaQA	Hellaswag	GSM8K	MATH	MBPP	HumanEval	
RAW	8.03	59.58	73.00	78.00	5.70	5.00	60.98	41.47
RAND	13.28	58.27	73.00	75.35	35.36	52.20	63.72	<u>53.02</u>
INSTRUCTION LEN	8.62	58.44	72.86	73.30	27.05	53.10	63.72	51.01
ALPAGASUS (Chen et al., 2024d)	13.67	57.94	73.04	73.90	32.30	51.40	63.41	52.24
INSTAG-C (Lu et al., 2024)	9.51	58.50	73.06	74.70	35.35	51.90	64.70	52.53
INSTAG-D (Lu et al., 2024)	12.87	57.48	72.80	74.40	33.75	51.80	64.02	52.45
SUPERFILTER (Li et al., 2024a)	19.16	58.98	72.99	73.70	30.10	52.40	58.85	52.31
DEITA-C (Liu et al., 2024b)	8.94	58.07	73.06	73.90	35.55	52.90	62.20	52.09
DEITA-Q (Liu et al., 2024b)	14.06	59.07	73.16	75.80	35.50	23.00	58.24	48.40
DEITA-D (Liu et al., 2024b)	16.41	57.80	72.70	76.10	29.05	52.40	64.63	52.73
<b>DAAR (Ours)</b>	16.88	57.58	73.03	75.40	38.1	52.00	64.94	<b>53.99</b>

Table 11. Performance of DAAR with baselines on Qwen2.5-7B across various benchmarks.

Qwen2.5-7B	Common Sense		Reasoning	Mathematics		Coding		Avg
	NQ	TriviaQA	Hellaswag	GSM8K	MATH	MBPP	HumanEval	
RAW	8.84	58.14	72.75	78.20	9.10	7.40	78.05	44.64
RAND	11.46	57.85	73.08	78.90	13.15	62.50	71.65	<u>52.65</u>
INSTRUCTION LEN	11.34	58.01	72.79	78.00	15.80	62.30	68.12	52.34
ALPAGASUS (Chen et al., 2024d)	10.40	57.87	72.92	77.20	18.75	61.80	65.55	52.07
INSTAG-C (Lu et al., 2024)	10.81	58.45	73.27	76.00	13.30	61.80	68.29	51.70
INSTAG-D (Lu et al., 2024)	11.08	58.40	72.79	76.40	16.40	62.90	70.43	52.63
SUPERFILTER (Li et al., 2024a)	13.54	58.51	72.89	79.30	11.35	39.50	65.25	48.62
DEITA-C (Liu et al., 2024b)	10.50	58.17	73.14	74.60	16.60	62.00	72.26	52.47
DEITA-Q (Liu et al., 2024b)	11.24	57.83	72.97	78.50	12.95	38.10	67.68	48.47
DEITA-D (Liu et al., 2024b)	10.48	57.81	73.05	77.20	15.25	52.90	69.21	50.84
<b>DAAR (Ours)</b>	15.83	58.65	72.48	80.20	16.70	64.20	68.29	<b>53.76</b>